MESOSCOPIC EFFECTS IN SUPERCONDUCTIVITY

ROSARIO FAZIO
Istituto di Fisica, Università di Catania
viale A. Doria 6, 95129 Catania, Italy

AND

GERD SCHÖN
Institut für Theoretische Festkörperphysik
Universtität Karlsruhe, 76128 Karlsruhe, Germany

1. Introduction

Several chapters in this book elaborate on the concepts of mesoscopic physics. This includes phase-coherent quantum transport combined with concepts from the macroscopic world such as reservoirs and dissipation, as well as single-electron effects. Mesoscopic physics is displayed in the electronic transport properties of small systems with spatial dimensions in the range of a few nanometers to micrometers, at low temperatures typically below 1 K. The progress in nano-fabrication allowed the controlled fabrication of these structures and led to an increased interest in this physics.

Characteristic for superconductivity is the macroscopic phase coherence of the order parameter and the supercurrent flow, as well as the modifications of quasiparticle properties by the energy gap. Superconductivity adds new degrees of freedom and makes the description of mesoscopic electron transport richer. On the other hand, typical superconducting properties are influenced by mesoscopic effects, e.g. by charging effects, and the question arises whether superconductivity persists in ultrasmall systems (see e.g. the chapter by Ralph *et al.* in this volume).

In this chapter we will investigate mesoscopic superconducting systems and heterostructures of normal metals and superconductors. We will first discuss in Section 2 in a few illustrative examples the single-electron and charging effects in superconducting tunnel junction systems. We show how, on the one hand, the superconducting gap influences single-electron tunneling and how, on the other hand, charging effects influence Andreev reflec-

tion processes. Cooper pairs can tunnel coherently; associated with their quantum dynamics is the 'macroscopic quantum tunneling' of the phase in low capacitance junctions (see e.g. the chapter of Devoret and Grabert in this volume). In junctions with even lower capacitance quantum mechanical superposition of charge states play a role. The combination of coherent Cooper pair tunneling, Andreev reflection, and quasiparticle tunneling leads to richly structured dissipative I-V characteristics.

We then turn in Section 3 to the properties of superconductor-normal metal heterostructures. The key words here are proximity effect and, again, Andreev reflection. It has been known for a long time that the proximity effect and the conversion between normal and supercurrents modifies the system properties over a finite length near the interfaces. Recent experiments could spatially resolve these properties either by probes placed close enough to the interface, or in samples with small spatial dimensions L, such that the Thouless energy D/L^2 becomes comparable to the temperatures in the experiment. We present some examples and several theoretical approaches to these physical questions.

2. Charging effects in low-capacitance superconducting junction systems

Modern technology has made it possible to fabricate, in a controlled way, metallic tunnel junctions with capacitances in the range of $C = 10^{-15}$F and below. In this case the charging energy associated with a single-electron charge, $E_{\rm C} \equiv e^2/2C$, is of the order of $10^{-4}e$V or larger, which corresponds to a temperature scale $E_{\rm C}/k_{\rm B} \geq 1$K. This implies that electron transport in the sub-Kelvin regime is strongly affected by charging effects (see the introductory chapter and Refs. [1, 2]).

If part of the system is superconducting further interesting effects are found: at subgap voltages single-electron tunneling (SET) is suppressed. This makes higher-order processes such as Andreev reflection in normal-superconductor (NS) junctions a dominant transport process. Here we discuss how this process is affected by the charging effects.

The charging energy allows the control of the electron number of small islands. Adding one electron to a small superconducting island necessarily puts it into an excited state with an energy exceeding the gap. Only when a second electron is added, can both recombine to form a Cooper pair. If this happens in a coherent way, the energy of the excitation created in the first tunneling process can be regained in the second. This leads to "parity effects", which distinguish between states with even or odd electron number in the superconducting island. As an example we analyze the I-V characteristics of a NSN SET transistor with a superconducting island

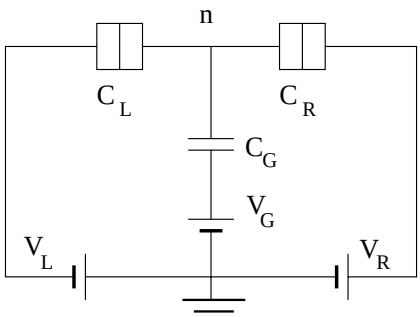

Figure 1. The SET transistor.

between normal conducting leads.

Also the coherent tunneling of Cooper pairs is influenced by charging effects. The charge and the phase difference in a Josephson junction, although macroscopic degrees of freedom, are quantum mechanical conjugate variables. The eigenstates in general are superpositions of different charge states. We discuss the consequences for the dissipative I-V characteristics of superconducting SET transistors. In an NSS transistor the Andreev reflection process in the NS junction can be used to probe the eigenstates emerging from coherent Cooper pair tunneling in the SS junction. In SSS transistors we analyze the combination of coherent Cooper pair tunneling and quasiparticle tunneling, which leads to richly structured I-V characteristic.

Reviews of single-electron effects in normal metal systems can be found in the book *Single Charge Tunneling* [2]. Tinkham's *Introduction to Superconductivity* [3] includes some topics of the present chapter. Recent work is presented in the proceedings of the workshop *Mesoscopic Superconductivity* [4] and reviews by Bruder [5] and Schön [6].

2.1. THE CHARGING ENERGY

The charging energy of systems of tunnel junctions depends on the electron number in various parts of the system and the applied voltages. An important example is the single-electron transistor shown in Fig. 1. An island is coupled via two tunnel junctions to a transport voltage source, $V = V_{\rm L} - V_{\rm R}$, such that a current can flow. The island is, furthermore, coupled capacitively to a gate voltage $V_{\rm G}$. The charging energy of the system depends on the integer number of excess electrons $n = \pm 1, \pm 2, ...$ on the island and the continuously varied voltages. Elementary electrostatics [2]

yields the "charging energy"

$$E_{\rm ch}(n,Q_{\rm G}) = \frac{(ne-Q_{\rm G})^2}{2C} \; . \tag{1}$$

Here $C = C_{\rm L}+C_{\rm R}+C_{\rm G}$ is the total capacitance of the island. The effect of the voltage sources is contained in the "gate charge" $Q_{\rm G} = C_{\rm G}V_{\rm G}+C_{\rm L}V_{\rm L}+C_{\rm R}V_{\rm R}$. Similar expressions hold for the "single-electron box", an even simpler system which consists of one junction only and a gate capacitance.

In a tunneling process, which changes the number of excess electrons in the island from n to $n+1$, the charging energy changes. Tunneling in the left junction is possible at low temperatures only if the energy in the left lead, $eV_{\rm L}$, is high enough to compensate for the increase in charging energy $eV_{\rm L} > E_{\rm ch}(n+1,Q_{\rm G}) - E_{\rm ch}(n,Q_{\rm G})$. Similarly, tunneling from the island (transition from $n+1$ to n) to the right lead is possible at low T only if $E_{\rm ch}(n+1,Q_{\rm G}) - E_{\rm ch}(n,Q_{\rm G}) > eV_{\rm R}$. Both conditions have to be satisfied simultaneously for a current to flow through the transistor. If this is not the case the current is exponentially suppressed, which is denoted as "Coulomb blockade". Varying the gate voltage produces the Coulomb oscillations, i.e. an e-periodic dependence of the conductance on $Q_{\rm G}$.

Many properties of the SET transistor and its extensions can be understood by considering only the energy of the different charge configurations. A further understanding of the I-V characteristic requires the knowledge of the tunneling rates of the electrons, which will be next topic.

2.2. SINGLE-ELECTRON TUNNELING RATES

The SET transistor, shown in Fig. 1, is described by the Hamiltonian

$$H = H_{\rm L} + H_{\rm I} + H_{\rm R} + H_{\rm ch} + H_{\rm t} \; . \tag{2}$$

Here, $H_{\rm L} = \sum_{k,\sigma} \epsilon_k c^\dagger_{k\sigma} c_{k\sigma}$ describes noninteracting electrons with wave vector k in the left lead, with similar expressions for the island (with states denoted by q) and the right lead. The Coulomb interaction, $H_{\rm ch} = (ne-Q_{\rm G})^2/(2C)$, is assumed to depend only on the total (net) charge $n = \sum_{k,\sigma} c^\dagger_{k\sigma} c_{k\sigma} - n_+$ on the island (electronic and ionic background), as discussed above. Charge transfer processes are described by a tunneling Hamiltonian, for instance tunneling in the left junction by

$$H_{\rm t,L} = \sum_{k,q,\sigma} T_{kq} c^\dagger_{k\sigma} c_{q\sigma} + {\rm h.c.} \; . \tag{3}$$

We determine the transition rates by Golden-rule arguments. An electron tunnels from one of the states k in the left lead into one of the available

states q in the island, thereby changing the electron number from n to $n+1$, with rate

$$\gamma_{\rm LI}(n) = \frac{1}{e^2 R_{\rm t,L}} \int_{-\infty}^{\infty} {\rm d}E \int_{-\infty}^{\infty} {\rm d}E' \mathcal{N}_{\rm L}(E)\mathcal{N}_{\rm I}(E') \times f_{\rm L}(E)[1-f_{\rm I}(E')] \quad \delta(E'-E+\delta E_{\rm ch}) \ . \quad (4)$$

The crucial point is that the conservation of energy, expressed by the δ-function, includes apart from the energies of the electron states $\epsilon_{k/q}$ also the charging energy. The latter depends on the change of the electron number and the applied voltages. In the process considered it changes by $\delta E_{\rm ch} = E_{\rm ch}(n+1,Q_{\rm G}) - E_{\rm ch}(n,Q_{\rm G}) - eV_{\rm L}$. We further introduced the normal state tunnel conductance of the junction $R_{\rm t,L}^{-1} = (4\pi e^2/\hbar) N_{\rm I}(0)\Omega_{\rm I} N_{\rm L}(0)\Omega_{\rm L}|T|^2$. At this stage, the tunnel matrix elements T_{kq} can be considered as constants; $N_{\rm I/L}(0)$ and $\Omega_{\rm I/L}$ denote the normal densities of states and volumes of the island and lead. If the electrodes are superconducting we have to account for the reduced densities of states. In ideal systems they take the BCS form $\mathcal{N}_{\rm I/L}(E) = \Theta(|E|-\Delta_{\rm I/L})\,|E|/\sqrt{E^2-\Delta_{\rm I/L}^2}$.

Usually the distribution functions $f_{\rm I/L}$ can be chosen to be Fermi functions. If both electrodes are normal conducting the integrals over the electron states in Eq. (4) can be performed, resulting in the "single-electron tunneling" (SET) rate [1]

$$\gamma_{\rm LI}(n,Q_g) = \frac{1}{e^2 R_{\rm t,L}} \frac{\delta E_{\rm ch}}{\exp[\delta E_{\rm ch}/k_{\rm B}T]-1} \ . \quad (5)$$

At low temperatures, $k_{\rm B}T \ll |\delta E_{\rm ch}|$, a tunneling process which would increase the charging energy is suppressed, $\gamma \to 0$. This phenomenon is called "Coulomb blockade" of electron tunneling.

If one or both electrodes are superconducting the rate still can be expressed in a transparent way

$$\gamma_{\rm LI}(n,Q_g) = \frac{1}{e} I_{\rm qp}\left(\frac{\delta E_{\rm ch}}{e}\right) \frac{1}{\exp[\delta E_{\rm ch}/k_{\rm B}T]-1} \ . \quad (6)$$

The function $I_{\rm qp}(V)$ is the well-known quasiparticle tunneling characteristic (see e.g. Ref. [3]), which is suppressed at voltages below the superconducting gap(s). Charging effects reduce the quasiparticle tunneling further. At zero temperature the rate is nonzero only if the gain in charging energy compensates the energy needed to create the excitations $\delta E_{\rm ch}+\Delta_{\rm I}+\Delta_{\rm L} \le 0$.

The rates describe the stochastic time evolution of the charge of the junction system. For the theoretical analysis Monte Carlo schemes or – in small systems – a master equation approach can be used. Examples of

the resulting I-V characteristics of normal metal junctions are presented in the introductory chapter of this volume. Characteristic is the e-periodic dependence of the current and conductance on the applied gate charge $Q_{\rm G}$. Examples of superconducting junction systems will be presented below.

2.3. TWO-ELECTRON TUNNELING, ANDREEV REFLECTION

In the regime where quasiparticle tunneling is suppressed by the superconducting gap higher-order processes involving multi-electron tunneling play a role. Cooper-pair tunneling is such a process, and will be discussed later. If only one of the electrodes is superconducting there still exists a 2-electron tunneling process, denoted as Andreev reflection[1]. In this process an electron approaching from the normal side with energy below the gap is reflected as a hole, while a Cooper pair propagates into the superconductor.

We will determine now the rate of Andreev tunneling taking into account charging effects, as discussed in Ref. [7]. For this purpose we consider a SET transistor with a superconducting island and normal leads (NSN). The tunneling Hamiltonian is rewritten in terms of the Bogoliubov creation and annihilation operators for the excitations in the superconducting island

$$H_{\rm t,L} = \sum_{k,q,\sigma} T_{kq}[u_{q,\sigma}\gamma^\dagger_{q,\sigma} + v^*_{q,\sigma}\gamma_{-q,-\sigma}]c_{k,\sigma} + \text{h.c.}\,. \tag{7}$$

Here, $u_{q,\sigma}$ and $v_{q,\sigma}$ are the standard BCS coherence factors with magnitudes $\sqrt{(1 \pm \epsilon_q/E_q)/2}$, and $E_q = \sqrt{\epsilon_q^2 + \Delta^2}$ is the energy of the quasiparticles.

Andreev reflection is a second-order coherent process. In the first part of the transition one electron is transferred from an initial state, e.g. $k\uparrow$ of the normal lead, into an intermediate excited state $q\uparrow$ of the superconducting island. In the second part of the coherent transition an electron tunnels from $k'\downarrow$ into the partner state $-q\downarrow$ of the first electron, such that both form a Cooper pair. The final state contains two excitations in the normal lead and an extra Cooper pair in the superconducting island. The amplitude for this process, to which we add the amplitude of the process in reverse order, is given by [7]

$$A_{kk'} = \sum_q T_{kq}T_{k'-q}u_q v_q \left(\frac{1}{\delta E_{\rm ch,1} + E_q - \epsilon_k} + \frac{1}{\delta E_{\rm ch,1} + E_q - \epsilon_{k'}}\right)\,. \tag{8}$$

Here spin indices have been suppressed and the relation $v_{q,\uparrow} = v^*_{q,\downarrow}$ has been used. The change in the charging energy $\delta E_{\rm ch,1} \equiv E_{\rm ch}(n+1, Q_{\rm G}) -$

[1] Andreev considered a normal metal and a superconductor in good metallic contact, but his physical picture can be generalized to tunnel junctions.

$E_{\rm ch}(n,Q_{\rm G})-eV$ corresponds to the virtual intermediate state where *one* electron has tunneled from the lead (at voltage V) to the island. Finally, the rate for the Andreev reflection process is

$$\gamma^A_{\rm LI}=\frac{2\pi}{\hbar}\sum_{k,k'}|A_{kk'}|^2\,f_{\rm L}(\epsilon_k)f_{\rm L}(\epsilon'_k)\delta(\epsilon_k+\epsilon'_k+\delta E_{\rm ch,2})\ . \tag{9}$$

Here, the change in the charging energy $\delta E_{\rm ch,2}=E_{\rm ch}(n+2,Q_{\rm G})-E_{\rm ch}(n,Q_{\rm G})-2eV$ corresponds to the real final state where *two* electron charges have been added to the superconducting island.

If we approximate the product of tunneling matrix elements by its average the q-summation in (8) can be performed, with the result $A_{kk'}=\pi N_{\rm I}(0)a\,(\Delta/\delta E_{\rm ch,1})\,\langle T_{kq}T_{k'-q}\rangle_q$, where $a(x)\equiv\frac{4}{\pi}\frac{x}{\sqrt{x^2-1}}\arctan\sqrt{\frac{x-1}{x+1}}$. Andreev reflection is most important if the gap Δ is larger than the relevant energy differences $|\delta E_{\rm ch,1}|$. In this limit the function a reduces to $a(x\gg1)\approx1$. Henceforth, we disregard this weak energy dependence: As such the integrations in (9) can be performed, resulting in

$$\gamma^A_{\rm LI}(n,Q_{\rm G})=\frac{G^{\rm A}}{4e^2}\frac{\delta E_{\rm ch,2}}{\exp(\delta E_{\rm ch,2}/k_{\rm B}T)-1}\ . \tag{10}$$

Note that the functional dependence of this rate coincides with that for single-electron tunneling in a normal junction, Eq. (5). Hence Andreev reflection is subject to Coulomb blockade like normal-state single-electron tunneling [8] with the exception that:
(i) The charge transferred in an Andreev reflection is $2e$, and the charging energy changes accordingly.
(ii) The effective Andreev conductance is of second-order in the tunneling conductance

$$G^{\rm A}=\frac{1}{4}\frac{R_{\rm K}}{N_{\rm ch}R_{\rm t}^2}\ . \tag{11}$$

(iii) We have to account for the number of independent parallel channels for both the normal state conductance, $1/R_{\rm t}=N_{\rm ch}/R_{\rm t,0}$, and the Andreev conductance, $G^{\rm A}\propto N_{\rm ch}R_{\rm K}/R_{\rm t,0}^2$. (Note that in Eq. (11) we express the latter by $1/R_{\rm t}$. Hence the factor $N_{\rm ch}$ appears in the denominator.) In the tunneling Hamiltonian approach $N_{\rm ch}$ is expressed by the correlations between the matrix elements [7]

$$\frac{1}{N_{\rm ch}}=\frac{\langle|\langle T_{kq}T_{k'-q}\rangle_q|^2\rangle_{k,k'}}{\left(\langle|T_{kq}|^2\rangle_{kq}\right)^2}\ . \tag{12}$$

A more detailed analysis [9] shows that the second-order Andreev process is sensitive to spatial correlations in the normal metal, which can be expressed

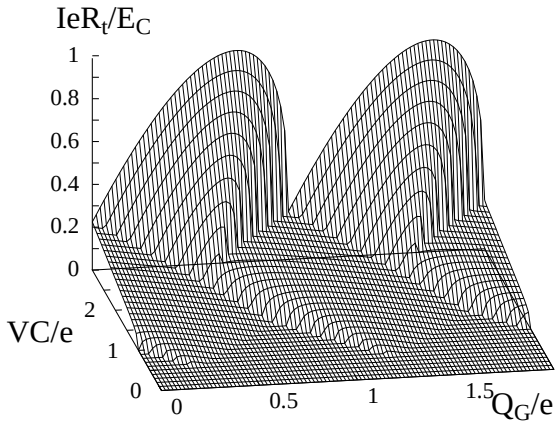

Figure 2. I-V characteristic of an NNS transistor. Both junctions have the same normal-state conductance. The ratio of Andreev and normal-state conductance is $G^{\rm A}R_{\rm t} = 0.02$, and $\Delta = 4E_{\rm C}$. From Ref. [10].

by the Cooperon propagator. For the moment we consider $N_{\rm ch}$ as a fit parameter; a comparison of the Andreev and the normal state conductance shows that even in small junctions it is much larger than one.

As an example we show in in Fig. 2 the I-V characteristic of a NNS SET transistor. The structure observed there with two characteristic scales arises due to a combination of single-electron tunneling with rate (6) and Andreev reflection with rate (10).

2.4. PARITY EFFECTS

2.4.1. *The Superconducting Electron Box*

In a normal-metal electron box, sweeping the applied gate voltage increases the electron number on the island in unit steps, and the voltage of the island shows a periodic saw-tooth behavior. The periodicity in the gate charge $Q_{\rm G}$ is e. If the island is superconducting and the gap Δ smaller than the charging energy $E_{\rm C}$, the charge and the voltage show at low temperatures a characteristic long-short cyclic, $2e$-periodic dependence on $Q_{\rm G}$. This effect arises because single-electron tunneling from the ground state, where all electrons near the Fermi surface of the superconducting island are paired, leads to a state where one extra electron – the "odd" one – is in an excited state [11]. In a small island, as long as charging effects prevent further tunneling, the odd electron does not find another excitation for recombination. Hence the energy of this state stays (at least metastable) above that of the equivalent normal system by the gap energy. Only at larger gate

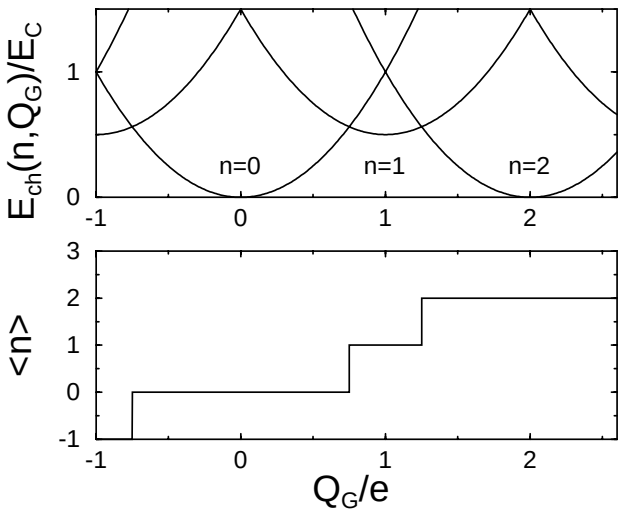

Figure 3. The charging energy of a superconducting single-electron box as a function of the gate voltage shows a difference between even and odd numbers n of electron charges on the island. Accordingly the average island charge $\langle n \rangle$ is found in a broader range of gate voltages in the even state than in the odd state.

voltages can another electron enter the island, and the system can relax to the ground state. This scenario repeats with periodicity $2e$ in $Q_{\rm G}$, as displayed in Fig. 3.

At low temperatures the even-odd asymmetry has been observed in the electron box [12] as well as in the I-V characteristics of superconducting SET transistors [13, 14, 15]. However, at higher temperatures, above a cross-over value $T_{\rm cr} \ll \Delta$, the e-periodic behavior typical for normal-metal systems is recovered. We can explain this cross-over as well as the structure in the I-V characteristics by analyzing the rate of tunneling of electrons between the lead and the island, paying particular attention to the fate of the "odd" electron [16, 17].

We first consider an electron box with a superconducting island and a normal lead. If the distribution functions of lead and island are Fermi functions, the rate of tunneling is given by Eq. (6). At low temperature the rate $\gamma_{\rm LI}$ is finite only at voltages where the gain in charging energy (i.e. $\delta E_{\rm ch} < 0$) exceeds the energy of the excitations ($\epsilon_k \geq 0, E_p \geq \Delta$) created in the lead and island, i.e. for $\delta E_{\rm ch} + \Delta < 0$. It is exponentially suppressed otherwise. The assumption of equilibrium Fermi distributions is sufficient when we start from the even state. For definiteness let us assume that we started from $n = 0$ at gate voltage $0 \leq Q_{\rm G} \leq e$. As such, the relevant change in charging energy is $\delta E_{\rm ch} = E_{\rm ch}(1, Q_{\rm G}) - E_{\rm ch}(0, Q_{\rm G})$ and the rate

of tunneling from an even to an odd state is given by eq. (6)

$$\gamma^{\rm eo} = \gamma_{\rm LI}(n=0, Q_{\rm G}) \ . \tag{13}$$

In the odd state the quasiparticle distribution differs from an equilibrium Fermi function. There is extra charge in the normal component. After thermalization the excitations in the island can be described by a Fermi function, $f_{\delta\mu}(\epsilon) = [{\rm e}^{(\epsilon-\delta\mu)/k_{\rm B}T}+1]^{-1}$, but with a shifted chemical potential $\mu_{\rm N} = \mu_{\rm S} + \delta\mu$ relative to the condensate. The shift in chemical potential is fixed by the constraint of *one* excess electron charge $1 = N_{\rm I}(0)\Omega_{\rm I}\int_{-\infty}^{\infty} {\rm d}E \mathcal{N}_{\rm I}(E)[f_{\delta\mu}(E) - f_0(E)]$. This reduces at low temperatures to

$$\delta\mu = \Delta - k_{\rm B}T \ln N_{\rm eff}(T), \tag{14}$$

where

$$N_{\rm eff}(T) = N_{\rm I}(0)\Omega_{\rm I}\sqrt{2\pi\Delta k_{\rm B}T} \tag{15}$$

is the number of states in the island available for quasiparticles near the gap [13]. Parity effects are observable as long as the shift of the chemical potential is relevant $\delta\mu > k_{\rm B}T$. This is the case for temperatures below the cross-over temperature

$$k_{\rm B}T_{\rm cr} = \Delta/\ln N_{\rm eff}(T_{\rm cr}) \ . \tag{16}$$

The tunneling rate back from the odd state (here $n=1$) to the even state ($n=0$), $\gamma^{\rm oe} = \gamma_{{\rm IL},\delta\mu}(n=1, Q_{\rm G})$, is given by (4) with the island distribution function replaced by $f_{\delta\mu}(\epsilon)$. For $\exp(-\Delta/k_{\rm B}T) \ll 1$ the ratio of the rates of the two transitions is

$$\gamma^{\rm oe}/\gamma^{\rm eo} = {\rm e}^{[E_{\rm ch}({\rm odd})+\delta\mu-E_{\rm ch}({\rm even})]/k_{\rm B}T} = {\rm e}^{\delta F/k_{\rm B}T} \ . \tag{17}$$

In other words, they obey a detailed balance relation, depending on a "free energy" difference, which, in addition to the charging energy, contains the shift of the chemical potential $\delta\mu$. This free energy difference coincides with that introduced in Ref. [13].

For the following discussion it is useful to decompose the rate as

$$\gamma^{\rm oe} = \gamma_{\rm IL}(1, Q_{\rm G}) + \delta\gamma(Q_{\rm G}) \ , \tag{18}$$

where $\gamma_{\rm IL}$ is given by the equilibrium form, equivalent to (6), and

$$\delta\gamma(Q_{\rm G}) = \frac{1}{e^2 R_{\rm t}} \int_{-\infty}^{\infty} d\epsilon_k \int_{-\infty}^{\infty} {\rm d}E \mathcal{N}_{\rm I}(E) \times [f_{\delta\mu}(E) - f_0(E)] \quad [1 - f_0(\epsilon_k)]\delta(\epsilon_k - E - \delta E_{\rm ch}) \tag{19}$$

describes the rate of tunneling of the odd, excited electron [16]. In the important range of parameters $\Delta+\delta E_{\rm ch} > k_{\rm B}T$ this "odd-electron tunneling rate" reduces to

$$\delta\gamma(Q_{\rm G}) = \frac{1}{2e^2 R_{\rm t} N_{\rm I}(0)\Omega_{\rm I}}\,, \tag{20}$$

whereas it is exponentially suppressed otherwise. It contains a small prefactor $1/N_{\rm I}(0)\Omega_{\rm I}$ as compared to $\gamma_{\rm IL}$. On the other hand, in the considered range of gate voltages – since the energy of the excitation in the island is regained in the tunneling process – $\delta\gamma$ is not exponentially suppressed. Hence it may be larger than $\gamma_{\rm IL}$.

In the range $0 \le Q_{\rm G} \le e$ tunneling connects the island states $n = 0$ and $n = 1$. The range $e \le Q_{\rm G} \le 2e$ can be treated analogously. The tunneling now connects the states $n = 1$ and $n = 2$. In this case, except for the single-electron tunneling processes which create further excitations with rate (6), one electron can tunnel into one specific state $(-k, -\sigma)$, the partner state of the excitation (k, σ) which is already present. Both condense immediately; the state with two excitations only exists virtually. The latter process occurs again with rate $\delta\gamma(Q_{\rm G})$. The symmetry implies $\gamma^{\rm eo/oe}(Q_{\rm G}) = \gamma^{\rm eo/oe}(2e - Q_{\rm G})$. Since the properties of the system are $2e$-periodic in $Q_{\rm G}$, we have provided a complete description for all gate voltage.

The sequential tunneling of charges between the island and the lead is described by a master equation for the occupation probabilities of the even and odd states $P_{\rm e}(Q_{\rm G})$ and $P_{\rm o}(Q_{\rm G})$,

$$\frac{dP_{\rm e}(Q_{\rm G})}{dt} = -\gamma^{\rm eo}(Q_{\rm G})P_{\rm e}(Q_{\rm G}) + \gamma^{\rm oe}(Q_{\rm G})P_{\rm o}(Q_{\rm G}) \tag{21}$$

with $P_{\rm e}(Q_{\rm G})+P_{\rm o}(Q_{\rm G}) = 1$. With $\gamma_\Sigma(Q_{\rm G}) = \gamma^{\rm oe}(Q_{\rm G})+\gamma^{\rm eo}(Q_{\rm G})$ the equilibrium solution follows to be $P_{\rm e(o)}(Q_{\rm G}) = \gamma^{\rm oe(eo)}(Q_{\rm G})/\gamma_\Sigma(Q_{\rm G})$. For $\gamma^{\rm oe} \gg \gamma^{\rm eo}$ we have $P_{\rm e}(Q_{\rm G}) \approx 1$, i.e. the system occupies the even state, while for $\gamma^{\rm eo} \gg \gamma^{\rm oe}$ the island is in the odd state.

The cross-over value $Q_{\rm cr}$ of the gate charge, where the system switches between the even and the odd state, is determined by the condition $P_{\rm e} \approx P_{\rm o}$, i.e. $\gamma^{\rm oe}(Q_{\rm cr}) \approx \gamma^{\rm eo}(Q_{\rm cr})$. At low temperatures this condition coincides with the condition that the energy is minimal, see Fig. 3. At finite, but low temperature we find

$$Q_{\rm cr}(T) = \frac{e}{2} + \frac{C}{e}\left[\Delta - k_{\rm B}T \ln N_{\rm eff}(T)\right], \tag{22}$$

where $N_{\rm eff}(T)$ was introduced in (15). This means the short plateaus in Fig. 3 get longer until, above $T_{\rm cr}$, we have $Q_{\rm cr} = e/2$, and the e-periodic behavior known from normal systems is recovered.

2.4.2. *I-V Characteristics of NSN Transistors*

The analysis presented above can be extended such that we can derive the I-V characteristics of SET transistors with a superconducting island. We first consider an NSN transistor with an energy gap smaller than the charging energy scale $\Delta < E_{\rm C}$. In this system the important processes are single-electron tunneling processes in the left and right junction, causing transitions between even and odd states, with rates $\gamma_{\rm L}^{\rm eo/oe}$ and $\gamma_{\rm R}^{\rm eo/oe}$ which are obvious generalizations of Eq. (13) and (18). At low T it is sufficient to consider only one even and one odd state of the island. The solution of the corresponding master equation yields the single-electron tunneling current

$$I = e(\gamma_{\rm L}^{\rm eo} P_{\rm e} - \gamma_{\rm L}^{\rm oe} P_{\rm o}) = e\frac{\gamma_{\rm L}^{\rm eo}\gamma_{\rm R}^{\rm oe} - \gamma_{\rm R}^{\rm eo}\gamma_{\rm L}^{\rm oe}}{\gamma_{\rm L}^{\rm eo} + \gamma_{\rm R}^{\rm eo} + \gamma_{\rm L}^{\rm oe} + \gamma_{\rm R}^{\rm oe}} \ . \tag{23}$$

At high temperatures, $T > T_{\rm cr}$, this current (23) shows the Coulomb oscillations known from normal systems with parabola-shaped maxima at the points $Q_{\rm G} = e/2 + ne$ with integer n. At low temperatures, $T < T_{\rm cr}$, the current is limited by the odd-electron tunneling rate γ in one of the junctions. In the window $Q_{\rm cr}(T) < Q_{\rm G} < \frac{e}{2} + \Delta C/e + Q_{\rm cr}/2 < e$ it is

$$I_{\rm plateau} = e\delta\gamma = \frac{1}{2eR_{\rm t}N_{\rm I}(0)\Omega_{\rm I}} \ , \tag{24}$$

while it is exponentially small outside. A second current plateau exists in the window $e < 3e/2 - \Delta C/e - Q_{\rm cr}/2 < Q_{\rm G} < 2e - Q_{\rm cr}$. Both plateaus create a double structure which repeats 2e-periodically. For $\Delta + eV/2 > E_{\rm C}$ the two plateaus merge to form a 2e-periodic single plateau structure. The resulting I-V characteristic is visualized in Fig. 4.

In NSN transistors with a larger superconducting gap $\Delta > E_{\rm C}$ the odd states have a large energy. Hence a mechanism which transfers two electrons between the normal metal and the superconductor becomes important. Andreev reflection with rate (10) provides such a mechanism [7]. The master equation description can be generalized to include also this process. At low temperatures a set of parabolic current peaks is found centered around the degeneracy points $Q_{\rm G} = \pm e, \pm 3e, \ldots$ [7]

$$I^{\rm A}(\delta Q_{\rm G}, V) = G^{\rm A}\left(V - 4\frac{\delta Q_{\rm G}^2}{VC^2}\right)\Theta\left(V - 4\frac{\delta Q_{\rm G}^2}{VC^2}\right) \ . \tag{25}$$

Here $\delta Q_{\rm G}$ is $\delta Q_{\rm G} = Q_{\rm G} - e$ for $Q_{\rm G}$ close to e, and similar near the other degeneracy points.

At larger transport voltages, single-electron tunneling sets in, even if $\Delta > E_{\rm C}$, and Andreev reflection gets "poisoned" [7]. This occurs for

$$V \geq V_{\rm poison} = \frac{2}{e}\left(E_{\rm C} - \frac{eQ_{\rm G}}{C} + \Delta\right) \ . \tag{26}$$

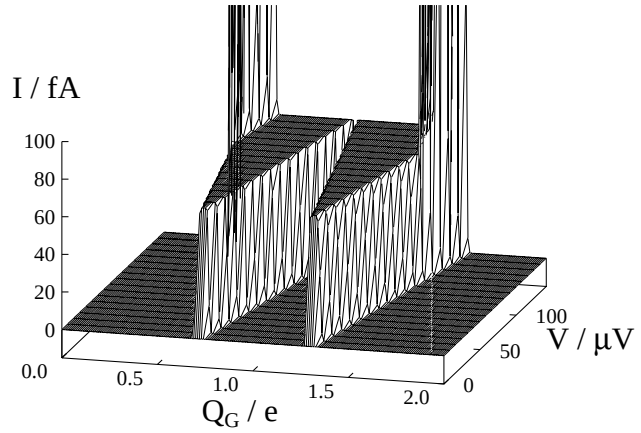

Figure 4. The current $I(Q_{\rm G}, V)$ through a NSN transistor with $\Delta < E_{\rm C}$. From Ref. [17].

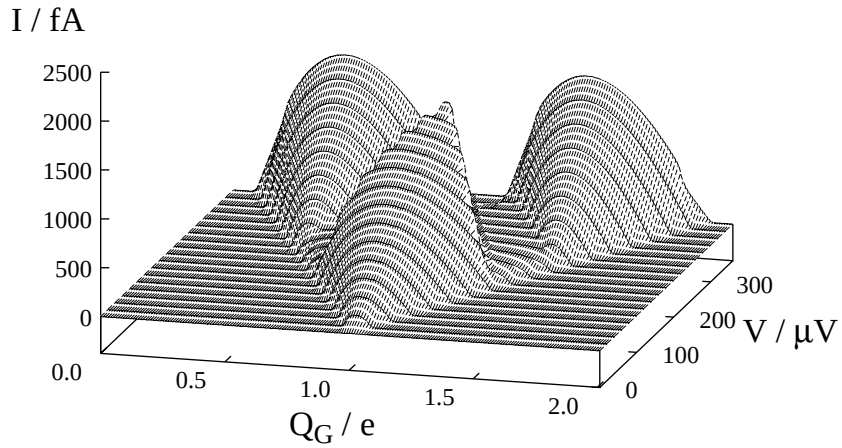

Figure 5. The current $I(Q_{\rm G}, V)$ through a NSN transistor with $\Delta > E_{\rm C}$. The parameters correspond to those of the experiments [15], $E_{\rm C} = 100\mu e$V, $\Delta = 245\mu e$V, $R_{\rm tl/R} = 43k\Omega, 1/G^{\rm A} \approx 1.2(2.4)10^8\Omega$ for the left (right) junction. From Ref. [17].

The rate for this transition, from the even to the odd state, is of the order of $\gamma^{\rm eo} \sim (V - V_{\rm poison})/eR_{\rm t}$. It puts the system into an excited state, making it energetically favorable that a second electron tunnels into the partner state of the excitation created in the first process. The rate for the second process is given by $\delta\gamma$, which in the considered range of parameters takes the value given in Eq. (20). Typically the rate for the second transition, from odd to even, is smaller than that of the first processes and, hence, creates the bottleneck in the sequence of SET processes. The same inequality

also implies that above $V_{\rm poison}$ the system is most likely in the odd state, $P_{\rm o}/P_{\rm e} = \gamma^{\rm eo}/\delta\gamma \gg 1$. Hence the current produced by the cycle is given by Eq. (24).

Fig. 5 shows the current-voltage characteristic of a NSN transistor with $\Delta > E_{\rm C}$. At small transport voltages the 2e-periodic peaks due to Andreev reflection dominate; they get poisoned above a threshold voltage. The peaks at larger transport voltages arise from a combination of single-electron tunneling and Andreev reflection. The shape and size of the even-even Andreev peaks and some of the single-electron tunneling features at higher transport voltages agree well with those observed in the experiments of Hergenrother et al. [15].

2.5. COOPER PAIR TUNNELING

2.5.1. *Macroscopic Quantum Effects*

In "classical" Josephson junctions, Cooper pairs can tunnel free of dissipation between the superconducting electrodes. The coupling is described by the Josephson energy $-E_{\rm J}\cos\varphi$, which depends on φ, the phase difference across the barrier. The energy scale $E_{\rm J} = \hbar I_{\rm cr}/2e$ is related to the critical current of the junction, which in turn can be expressed by the tunneling resistance of the junction and the energy gap of the superconductor, $I_{\rm cr}(T=0) = \pi\Delta/(2eR_{\rm t})$.

Charging effects introduce quantum dynamics: The phase difference and the charge on the electrodes, Q, are quantum mechanical conjugate variables. An ideal Josephson junction is governed by the Hamiltonian

$$H_0 = \frac{Q^2}{2C} - E_{\rm J}\cos\varphi \quad , \quad Q = \frac{\hbar}{\rm i}\frac{\partial}{\partial(\hbar\varphi/2e)} \; . \tag{27}$$

(For simplicity, we first describe a single junction; generalizations are presented below.) An important question, addressed in Refs. [18, 19, 20, 21], is how to account for dissipation due to the flow of normal currents and/or quasiparticle tunneling. The so-called "macroscopic quantum effects" like macroscopic quantum tunneling of the phase, or quantum coherent oscillations are derived from the Hamiltonian (27). Macroscopic quantum tunneling has been observed in tunnel junctions with small capacitances of the order of 10^{-12} F. These values are still orders of magnitude to large for single-electron effects to play a role.

2.5.2. *Superposition of Charge States*

We now turn to mesoscopic Josephson junctions or junction systems, where the number of electrons or Cooper pairs in small islands is the relevant degree of freedom. The charging energy has been discussed above. The

Josephson coupling describes the transfer of Cooper-pair charges forward or backward, and can be written in a basis of charge states as

$$\langle n|E_{\rm J}\cos\varphi|n'\rangle = \frac{E_{\rm J}}{2}(\delta_{n',n+2}+\delta_{n',n-2})\ . \tag{28}$$

Below, we will consider situations where Cooper pairs tunnel coherently, which shows features known from the phenomenon of resonant tunneling. Coherent Cooper pair tunneling is non-dissipative and strongest near points of degeneracy. First we will show that these quantum fluctuations broaden the steps in the expectation value of the charge on the island of a superconducting electron box. Then we will discuss how coherent Cooper-pair tunneling can be probed by Andreev reflection and observed in the dissipative I-V characteristic of a NSS transistor [22]. Finally we describe how the combination of coherent Cooper-pair tunneling and dissipative quasiparticle tunneling leads to a dissipative I-V characteristic of SSS transistors [23, 24, 13, 25, 26]. Further examples of coherent tunneling of Cooper pairs can be found in the literature, e.g. the gate-voltage dependence of the critical current of SSS or SNS transistors [27, 28].

We first consider an electron box with superconducting island and lead with large energy gap at low temperatures, $\Delta > E_{\rm C} \gg k_{\rm B}T$. In this case, at low voltages, quasiparticle tunneling is suppressed, and the island charge can change only by Cooper-pair tunneling in units of $2e$ as described by Eq. (28). The tunneling is strong near points of degeneracy. For instance for $Q_{\rm G} \approx e$ the charging energies of the states with $n = 0$ and $n = 2$ are comparable, and we can restrict our attention to these two charge states. The coherent tunneling between both is described by the 2×2 Hamiltonian

$$H = \begin{pmatrix} E_{\rm ch}(0) & -E_{\rm J}/2 \\ -E_{\rm J}/2 & E_{\rm ch}(2) \end{pmatrix}\ . \tag{29}$$

This Hamiltonian is easily diagonalized: the eigenstates and energies are

$$\begin{aligned} \psi_0 &= \alpha|0\rangle + \beta|2\rangle \quad , \quad \psi_1 = \beta|0\rangle - \alpha|2\rangle\ , \\ \alpha^2 &= \frac{1}{2}\Big[1+\frac{\delta E_{\rm ch}}{\sqrt{\delta E_{\rm ch}^2+E_{\rm J}^2}}\Big] = 1-\beta^2\ , \\ E_{0/1} &= \frac{1}{2}\left[E_{\rm ch}(0)+E_{\rm ch}(2) \mp \sqrt{\delta E_{\rm ch}^2+E_{\rm J}^2}\right]\ . \end{aligned} \tag{30}$$

Here we have introduced the difference in charging energy $\delta E_{\rm ch} \equiv E_{\rm ch}(2) - E_{\rm ch}(0) = 4E_{\rm C}\,(Q_{\rm G}/e-1)$. The coefficient α approaches unity if the charging energy of the state $|2\rangle$ lies far above that of $|0\rangle$, i.e. for $\delta E_{\rm ch} > 0$, and vanishes in the opposite limit, while β has the complementary behavior.

The expectation value of the charge on the island in the ground state is given by

$$\langle\psi_0|n|\psi_0\rangle = 2\beta^2 \ . \tag{31}$$

It changes near $Q_{\rm G} = e$ from 0 to 2 over a width of order $\delta Q_{\rm G} \approx E_{\rm J}/E_{\rm C}$. This has recently been observed experimentally [29].

2.5.3. *NSS Transistors*

Next we consider a NSS transistor. In this system the coherent tunneling of Cooper pairs in the Josephson (SS) junction can be probed by the dissipative current due Andreev reflection across the NS junction [22]. We restrict ourselves to low temperatures, $k_{\rm B}T \ll E_{\rm J}$. In order to describe coherent Cooper-pair tunneling in a situation with nonzero transport voltage we have to account in the Hamiltonian for the work done by the voltage sources during the transitions. We, therefore, keep track also of the number of electrons $N_{\rm L}$ and $N_{\rm R}$ in the left and right electrode. A basis set of states is denoted by $|N_{\rm L}, n, N_{\rm R}\rangle$, and the corresponding charging energy (for symmetric bias $V_{\rm L} = -V_{\rm R} = V/2$) is

$$H_{\rm ch}(N_{\rm L}, n, N_{\rm R}) = (ne - Q_{\rm G})^2/2C - (N_{\rm R} - N_{\rm L})eV/2 \ . \tag{32}$$

In a situation where only two charge states get appreciably mixed the eigenstates and energies of the corresponding 2×2 Hamiltonian are

$$\begin{aligned} \psi_0 &= \alpha|0,0,0\rangle + \beta|0,2,-2\rangle \quad , \quad \psi_1 = \beta|0,0,0\rangle - \alpha|0,2,-2\rangle \ , \\ E_{0/1} &= \frac{1}{2}\left[E_{\rm ch}(0,0,0) + E_{\rm ch}(0,2,-2) \mp \sqrt{\delta E_{\rm ch}^2 + E_{\rm J}^2}\right] \ . \end{aligned} \tag{33}$$

The coefficients coincide with those of the box discussed above, except for the obvious change of notation, and $\delta E_{\rm ch} = E_{\rm ch}(0,2,-2) - E_{\rm ch}(0,0,0)$.

In the low-bias regime, the dominant mechanism of transport in the NS junction of the transistor is Andreev reflection. Starting from a state $|0,0,0\rangle$ we are led in such a process to the state $|-2,2,0\rangle$. The Josephson coupling mixes this state with the state $|-2,0,2\rangle$. Hence we have to consider a second set of eigenstates

$$\psi_0' = \alpha|-2,0,2\rangle + \beta|-2,2,0\rangle \quad , \quad \psi_1' = \beta|-2,0,2\rangle - \alpha|-2,2,0\rangle \ . \tag{34}$$

The coefficients α and β are the same as for the other pair, but the corresponding energies are shifted $E_{0/1}' = E_{0/1} - 2eV$.

Andreev reflection causes transitions between the two set of eigenstates $\psi_0 \to \psi_0'$. The rate for this process can be derived along the lines described in an earlier. Compared to Eq. (8) a modification arises since the charge transfer operators pick from the initial state the component with

zero charge on the island, which has amplitude α, and select from the final state the component with two extra charges, which has amplitude β. Hence the amplitude for a Andreev reflection process between the states ψ_0 and ψ_0' with two electrons tunneling from the states $k,\uparrow$ and $k',\downarrow$ of the normal electrode is

$$A_{k,k'}(\psi_0 \to \psi_0') = \alpha\beta \sum_q T_{kq} T_{k'-q} u_q v_q \left(\frac{1}{E_0 - E_{kq}} + \frac{1}{E_0 - E_{k'q}} \right) . \quad (35)$$

The energy of the virtual intermediate state $|-1_k, 1_q, 0\rangle$, with one electron added to the island and two excited quasiparticles with energies ϵ_k and $E_q = \sqrt{\epsilon_q^2 + \Delta^2}$ in the normal and superconducting electrode, is given by $E_{kq} = E_{\rm ch}(-1,1,0) - \epsilon_k + E_q$.

The summation in Eq. (35) can be performed, and the rate for the Andreev reflection process is obtained by the Golden rule. After summation over the initial states k and k' one finds for $E_0' - E_0 = -2eV \leq 0$

$$\gamma(\psi_0 \to \psi_0') = (\alpha\beta)^2 \, a_0^2 \, \frac{G^{\rm A}}{4e^2} \, 2eV \ . \quad (36)$$

The rate is proportional to the product

$$\alpha^2 \beta^2 = \frac{1}{4} \frac{E_{\rm J}^2}{(\delta E_{\rm ch})^2 + E_{\rm J}^2} \ , \quad (37)$$

which displays a typical resonance structure. Here $G^{\rm A}$ is the Andreev conductance (11),and the function $a_0 = a\,(\Delta/[E_{\rm ch}(-1,1,0) - E_0])$ has been defined below Eq. (9). We further assumed that the energy $\Delta + E_{\rm ch}(-1,1,0)$ of the intermediate state lies above E_0. If $\Delta \gg E_{\rm C}$ the function a_0 reduces to $a_0 \approx 1$.

Andreev reflection processes can also lead to transitions between the other states introduced above, with rates

$$\begin{aligned}
\gamma(\psi_0 \to \psi_1') &= \alpha^4 \, a_0^2 \, \frac{G^{\rm A}}{4e^2} \, [E_0 + 2eV - E_1] \, \Theta[E_0 + 2eV - E_1)] \ , \\
\gamma(\psi_1 \to \psi_0') &= \beta^4 \, a_1^2 \, \frac{G^{\rm A}}{4e^2} \, [E_1 + 2eV - E_0] \ , \\
\gamma(\psi_1 \to \psi_1') &= (\alpha\beta)^2 \, a_1^2 \, \frac{G^{\rm A}}{4e^2} \, 2eV \ . \quad (38)
\end{aligned}$$

The function a_1 is defined similar as a_0, but the energy of the initial state E_0 is replaced by E_1.

Below the threshold voltage $V < V_{\rm th} = (E_1 - E_0)/2e$ the only transition at low temperatures is Andreev reflection between the states ψ_0 and ψ_0'.

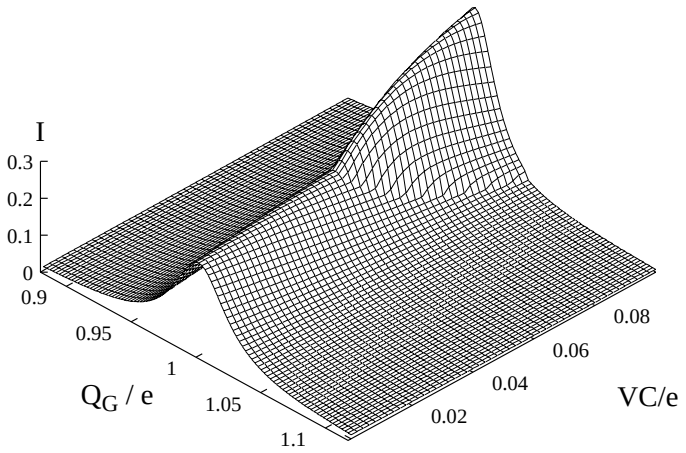

Figure 6. I-V characteristic of a NSS transistor. A resonant structure due to Cooper pair tunneling is visible in the dissipative current due to Andreev reflection. From Ref. [22].

The resulting current, $I = 2e\gamma(\psi_0 \to \psi_0')$, shows a pronounced resonant structure due to the overlap of the functions α and β. At higher voltages Andreev reflection can take the transistor to the excited state ψ_1'. A master equation yields the probabilities for the ground and excited states

$$P_0 = \frac{\gamma(\psi_1 \to \psi_0')}{\gamma(\psi_0 \to \psi_1') + \gamma(\psi_1 \to \psi_0')} \ , \ P_1 = 1 - P_0 \neq 0 \ \text{ for } \ V > V_{\rm th} \ . \quad (39)$$

The current then is

$$\frac{I}{2e} = [\gamma(\psi_0 \to \psi_0') + \gamma(\psi_0 \to \psi_1')]\, P_0 + [\gamma(\psi_1 \to \psi_1') + \gamma(\psi_1 \to \psi_0')]\, P_1 \ . \quad (40)$$

A plot of the current-voltage-characteristic, as a function of the gate and bias voltage is shown in Fig. 6 for the case where the superconducting gap is larger than the charging energy $\Delta \geq E_0$.

2.5.4. *SSS Transistors*

Next we consider the case of an SSS-SET transistor with superconducting electrodes and island below the crossover temperature $T_{\rm cr}$ where parity effects can be observed. The charging energy and coherent Cooper pair tunneling in this system are described by the model Hamiltonian [24]

$$H_0 = \sum_{n,\bar{n}} \left(\left[\frac{(ne - Q_{\rm G})^2}{2C} - \frac{1}{2} e\bar{n}V \right] |n, \bar{n}\rangle\langle n, \bar{n}| \right.$$
$$\left. - \frac{E_J}{2} \sum_{\pm} \sum_{\pm} |n \pm 2, \bar{n} \pm 2\rangle\langle n, \bar{n}| \right) \ . \quad (41)$$

Here we shortened the notation as compared to the previous subsection Eq. (32) and introduced $\bar{n} \equiv (N_{\rm R} - N_{\rm L})$, the number of electrons which have tunneled through the transistor. The eigenstates of H_0 are linear combinations of different charge states

$$|\Psi_\alpha\rangle = \sum_{n,\bar{n}} a^\alpha_{n,\bar{n}} |n,\bar{n}\rangle \quad , \tag{42}$$

and the energies are E_α.

Quasiparticle tunneling can cause transitions between different eigenstates $|\Psi_\alpha\rangle$. It is accounted for by

$$\begin{aligned} H_{\rm t}^{\rm qp} &= \sum_{k\in{\rm L},q\in{\rm I}} T^{({\rm L})}_{kq} |n+1,\bar{n}+1\rangle\langle n,\bar{n}| c_q^\dagger c_k + {\rm h.c.} \\ &+ \sum_{q\in{\rm I},k'\in{\rm R}} T^{({\rm R})}_{qk'} |n-1,\bar{n}+1\rangle\langle n,\bar{n}| c_{k'}^\dagger c_q + {\rm h.c.}\ . \end{aligned} \tag{43}$$

If the junction resistances are large compared to the quantum resistance $R_{\rm t,L/R} > R_{\rm K} = h/e^2$ the transition rates can be calculated by the Golden rule. A quasiparticle tunneling process in the left junction gives rise to a transition with rate

$$\gamma^{({\rm L})}_{\alpha\to\beta} = \sum_{n,\bar{n},\pm} \left(\frac{I^{({\rm L})}_{\rm qp}(\varepsilon_{\alpha\beta})/e}{1-\exp(-\varepsilon_{\alpha\beta}/k_{\rm B}T)} + \gamma \right) |\langle\Psi_\beta|n\pm1,\bar{n}\pm1\rangle\langle n,\bar{n}|\Psi_\alpha\rangle|^2 \ . \tag{44}$$

Here $I^{({\rm L})}_{\rm qp}$ is the I-V characteristic for quasiparticle tunneling in the left junction [3], and $\varepsilon_{\alpha\beta} = E_\alpha - E_\beta$ is the energy difference between initial and final state. We describe parity effects by including the escape rate $\delta\gamma$ of an odd quasiparticle in the island. It is given by an expression similar to Eq. (20), modified by the density of state in the superconducting electrode. It is

$$\delta\gamma \simeq \frac{1}{2e^2 R_{\rm t} N_{\rm I}(0)} \frac{\varepsilon_{\alpha\beta}+\Delta}{\sqrt{(\varepsilon_{\alpha\beta}+\Delta)^2-\Delta^2}} \theta(\varepsilon_{\alpha\beta}) \tag{45}$$

if n is odd and vanishes in the even state.

In order to determine the dc-current we follow the procedure described in Ref. [26] and first determine the eigenstates of H_0, either in an expansion in the Josephson coupling or numerically taking into account a sufficient number of charge states. This procedure converges for not too large Josephson coupling energies, $E_{\rm J} < E_{\rm C}$. Given the eigenstates $|\Psi_\alpha\rangle$ we calculate the rates in Eq. (44), which then enter a master equation $\partial_t P_\alpha = \sum_{\beta\neq\alpha} (P_\beta \gamma_{\beta\to\alpha} - P_\alpha \gamma_{\alpha\to\beta})$ for the probabilities P_α to find the system in the α-th eigenstate. The stationary solution $\partial_t P_\alpha = 0$ is sufficient

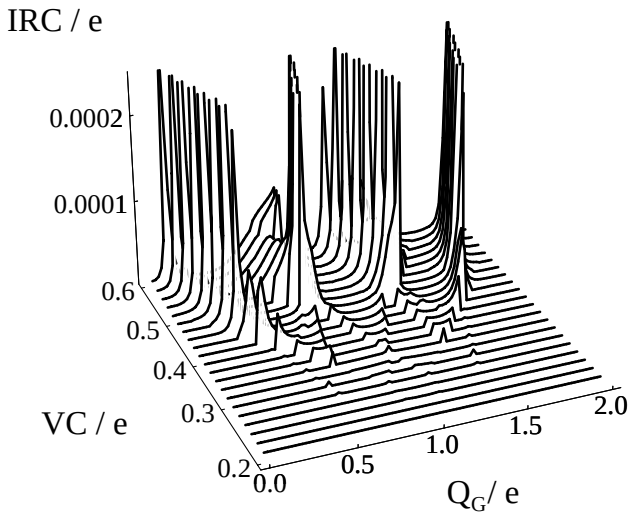

Figure 7. I-V characteristic of an SSS transistor. The parameters are $\Delta = 1.3E_{\rm C}$, $E_{\rm J} = 0.17E_{\rm C}$, $R_{\rm l/r} = R \approx R_{\rm K}$, $\gamma = 2.5 \cdot 10^{-5}(RC)^{-1}$. From Ref. [26].

to evaluate the dc-current

$$I = \frac{e}{2} \sum_{\alpha,\beta\neq\alpha} P_\alpha \gamma_{\alpha\to\beta} \left(\langle \Psi_\beta | \bar{n} | \Psi_\beta \rangle - \langle \Psi_\alpha | \bar{n} | \Psi_\alpha \rangle \right) \quad . \tag{46}$$

The combination of coherent Cooper pair tunneling and single-electron tunneling leads to a dissipative I-V characteristic. Results are shown in Fig. 7 with parameters corresponding to those in Ref. [13]. We note that the I-V characteristic is $2e$-periodic and observe a rich structure deep in the subgap region. For transport voltages $eV \gtrsim 2.5E_{\rm C}$ the $2e$-periodic features disappear and the current becomes e-periodic in $Q_{\rm G}$ again. This is not surprising since on a current scale $I \gg e\delta\gamma$ the unpaired quasiparticle in the island looses its importance.

For the parameters chosen at low transport voltages only few (two or three) states $|\Psi_\alpha\rangle$ are noticeably populated. Therefore, we can calculate the eigenstates of H_0, i.e. the coefficients $a^\alpha_{n,\bar{n}}$ in Eq. (42), by expanding in E_J. Away from certain resonant situations, the α-th eigenstate has only one coefficient $a^\alpha_{n,\bar{n}}$ of order unity, whereas all other coefficients are considerably smaller. To fix ideas, let us consider the state $|\Psi_0\rangle$ in the range of gate charges $Q_{\rm G} \in [0, e/2]$. In this eigenstate the most likely charge state is $|n = 0, \bar{n} = 0\rangle$, i.e. $a^0_{0,0} \approx 1$. Due to coherent tunneling of one Cooper pair, there is a non-zero amplitude $a^0_{\pm 2,\pm 2} \propto E_{\rm J}/E_{\rm C}$ for the system to be in the charge states $|n = \pm 2, \bar{n} = \pm 2\rangle$. Higher order Cooper pair tunneling leads to

a population of higher charge states with smaller amplitude. Off resonance the system is in the charge state $|2,6\rangle$ with amplitude $a^0_{2,6} \propto (E_\mathrm{J}/E_\mathrm{C})^3$.

At resonance these amplitudes are much larger. For instance along the line

$$3eV = 4E_\mathrm{C}(1 - Q_\mathrm{G}) \tag{47}$$

the charge states $|0,0\rangle$ and $|2,6\rangle$ have the same energy, and a three-Cooper-pair tunneling process is in resonance. As a result the amplitude is drastically increased $a^0_{2,6} \propto (E_\mathrm{J}/E_\mathrm{C})$.

A transition from $|\Psi_0\rangle$ to another eigenstate can occur if it is energetically favorable and the matrix element Eq. (44) is nonzero. When analyzing the energies we find that the process

$$|\Psi_0\rangle \approx |0,0\rangle \longrightarrow |\Psi_1\rangle \approx |1,7\rangle \qquad \text{(process a)}$$

is possible. Off resonance the rate of process a) is of the order $\gamma_{(\mathrm{a})} \propto (E_\mathrm{J}/E_\mathrm{C})^6$. However, in a narrow strip of width is proportional to E_J around the resonance line (47) we find

$$\gamma_{(\mathrm{a})} \propto \left(\frac{E_\mathrm{J}/2}{4E_\mathrm{C}(1-Q_\mathrm{G})+eV}\right)^2 \propto \left(\frac{E_\mathrm{J}}{E_\mathrm{C}}\right)^2 \quad . \tag{48}$$

This process leads to the most significant resonance in the I-V characteristic. We are, thus, led to the conclusion that the dominant transport process in the subgap region is tunneling of a quasiparticle accompanied by simultaneous tunneling of 3 Cooper pairs. This combination provides enough energy to overcome the quasiparticle tunneling gap 2Δ. The importance of this type of transport mechanism was first noted by Fulton *et al.* [23].

So far we have studied the conditions for the system to leave the initial state. However, a dc charge transport through the system requires cycles, after which the island returns to a state equivalent to the initial one. The simplest version is a two-step cycle of subsequent transitions of the same type in the left and right junction. Such cycles dominate in NNN or NSN transistors at low bias voltages. The cycle which leads to the pronounced feature in Fig. 7, at $3eV = 4E_\mathrm{C}(1 - Q_\mathrm{G})$, arise due to two-step cycles as well, but the second step is different from the first one. The transition completing the cycle which starts with process a) is

$$|\Psi_1\rangle \approx |1e,7\rangle \longrightarrow |\Psi_2\rangle \approx |0,12\rangle \qquad \text{(process b)} \quad .$$

This means a quasiparticle transfer is accompanied by 2 Cooper-pair tunneling processes. The latter process is not in resonance and, therefore, the rate is $\gamma_{(\mathrm{b})} \propto (E_\mathrm{J}/E_\mathrm{C})^4$. Whereas off resonance the process a) is the bottleneck for the current, at resonance the process b) has the smaller rate. This explains the value of the current at the resonance.

For further discussions of the structures manifest in Fig. 7, including extensions such as the influence of fluctuations of the electromagnetic environment, as well as a comparison with experiments on SSS transistor [13, 28] we refer to Ref. [26].

2.6. EXTENSIONS

In the examples discussed above, the charging energy is the dominant energy, while tunneling could be described in low order perturbation theory or – in the case of coherent Cooper pair tunneling – by diagonalization of a simple Hamiltonian. The expansion parameter is the dimensionless tunneling conductance $R_{\rm K}/(4\pi^2 R_{\rm t})$, where $R_{\rm K} = h/e^2 = 25.8k\Omega$ is the quantum of the resistance. In situations where this parameter is not small a more general approach is required. H. Schoeller describes in his Chapter of this volume a diagrammatic expansion to account for strong tunneling through quantum dots [30, 31]. Strong tunneling in normal metal junctions has been studied by several authors [32, 33, 34, 35].

A formulation in terms of path integrals displays in a transparent way the interplay of charging effects and tunneling phenomena [31, 34]. Here we would like to draw attention to the equivalent path-integral description of superconducting junction systems, presented in Refs. [5, 6, 36]. In these articles applications to selected problems have been discussed, such as (i) the influence of charging effects on the Josephson current through a SNS system, where earlier results of Bauernschmitt *et al.* [37] have been reproduced, (ii) the influence of charging effects on Andreev reflection, and the proximity effect, which extends earlier results of Aslamazov *et al.* [38].

3. Hybrid Normal-Metal/Superconductor Structures

3.1. REVIEW

In the last few years new experiments revived the interest in equilibrium and non-equilibrium properties of superconductor-normal metal (SN) hybrid structures. Two key words in this context are: *proximity effect* and *Andreev reflection*. The hybrid structures can be grouped in two classes depending on the transparency of the interface between superconductor and normal metal. If they are separated by an insulating barrier with low transparency the process of two-electron tunneling is the relevant transport mechanism at low bias. If they are in good metallic contact nearly all particles are transmitted; here the dominant process is Andreev reflection. Various excellent reviews [39, 40, 5] discuss many aspects of SN structures. Our aim here is to introduce the basic concepts and theoretical techniques, and to review some of the current literature. Some examples are discussed

explicitly to demonstrate the physics involved.

When a superconductor is put in contact with a normal metal, Cooper pairs can leak across the interface. As a result there exists a non-vanishing pair amplitude in the normal metal, defined by

$$F(\vec{r}) = \langle \psi_\uparrow(\vec{r}) \psi_\downarrow(\vec{r}) \rangle \ , \tag{49}$$

where $\psi_\sigma(\vec{r})$ is the annihilation operator for an electron with spin σ. The pair amplitude is a two-particle property, related to the probability of finding two time-reversed electrons at position $\vec{r}$. The decay of $F(\vec{r})$ away from the interface depends strongly on properties – diffusive vs. ballistic, noninteracting vs. interacting – of the normal metal [41]. At finite temperature it decays in the normal metal exponentially on a scale ξ_T given by

$$\xi_T = \frac{\hbar v_{\rm F}}{2\pi T} \qquad \text{or} \qquad \sqrt{\frac{\hbar D}{2\pi T}} \ , \tag{50}$$

depending on whether the metal is in the clean or diffusive limit. Here D is the diffusion constant. (Henceforth, we use units where $\hbar = k_{\rm B} = 1$.) At zero temperature, if interaction effects can be be disregarded, the decay follows a power law, $F(\vec{r}) \propto 1/r$. The appearance of the pair amplitude on the normal side of the interface is accompanied by a depression of the order parameter on the superconducting side.

A nonvanishing pair amplitude implies the coherence of two electrons in the normal metal induced by the coupling to the superconductor. It does not necessarily lead to a gap in the spectrum, $\Delta(\vec{r}) = \lambda F(\vec{r})$, since both are related by the interaction strength λ, which may vanish in normal metals in the absence of an attractive or repulsive interaction.

The proximity effect is intimately related to the microscopic mechanism which governs the transport through SN interfaces. At voltages and temperatures below the superconducting gap single particle tunneling is exponentially suppressed. The dominant process is then Andreev reflection [42], where an incoming quasi-electron from N is reflected at the interface as a quasi-hole, as a result of which a Cooper pair is injected into the superconductor. The reflected hole has a momentum which is opposite (to order $|k - k_{\rm F}|/k_{\rm F}$) to the one of the incident electron. The small difference in the momentum implies that the particle and the hole maintain their phase coherence up to distance of the order of $L_\epsilon \sim \sqrt{D/\epsilon}$ where ϵ is the energy of the particle relative to the Fermi energy. If ϵ is the thermal energy, this length coincides with the correlation length given in Eq. (50) [43]. This demonstrates that the proximity effect and Andreev reflection, though seemingly different concepts, are closely related. Also in the presence of a tunnel barrier at the NS boundary the dominant mechanisms of transport

is the transfer of two electrons across the barrier. We call also this process Andreev tunneling, although the momentum perpendicular to the interface is not conserved. Andreev processes are also responsible for the Josephson effect in S-N-S sandwiches [38, 44]. If the thickness of the normal region is comparable to or less than its coherence length $\xi_{T,\mathrm{N}}$, phase coherence can be maintained and a supercurrent can flow through it, depending on the phase difference of the two superconductors.

Although many properties of hybrid SN system have already been studied in the past, the interest in proximity devices has been renewed recently. The reason is that it became possible to study mesoscopic hybrid systems with dimensions smaller than ξ_T. In this case the particle and the hole preserve their phase coherence across the entire conductor. Another relevant length scale, the phase-coherence length L_ϕ of single electrons in a normal metal, might well be larger than ξ_T.

In mesoscopic proximity systems the interplay between phase-coherent electron propagation in N and macroscopic phase coherence in S gives rise to interesting new physics [4]. For instance, Andreev reflection in mesoscopic N-S tunnel junctions is strongly influenced by electronic interference. The transport through NS-QUIDS (Normal Metal-Superconductor QUantum Interference DeviceS) was studied theoretically by Hekking and Nazarov [9] and experimentally by the Saclay group [45], showing the existence of a modulated current as a function of the flux piercing the device. Nakano and Takayanagi [46] considered a different type of interferometer where the phase difference is created by a current which passes through the superconductor. Petrashov *et al.* [47] and Courtois *et al.* [48] performed a series of experiments on interference effects in transport through mesoscopic samples containing superconducting arms. Proximity systems with clean N-S interfaces show a remarkable non-monotonic temperature dependence [49, 43]. In these systems the presence of the superconductor renders the diffusion constant of the normal metal effectively energy dependent.

Since electrons from the normal metal can enter the superconductor and then return to the normal metal not only the *off-diagonal* properties of the metal are modified, but also the single particle properties (*diagonal* in the Nambu space). Very recently, the local electron density of states (DOS) of a normal metal in contact with a superconductor has been studied at mesoscopic distances from the N-S interface [50, 51]. Close to the Fermi energy, a suppression of the DOS below its normal value has been observed.

Due to the development of superconductor-semiconductor (S-Sc) integration technology, it is now possible to observe the transport of Cooper pairs through S-Sc mesoscopic interfaces as well [4]. Examples are the supercurrent through a two-dimensional electron gas (2DEG) with Nb contacts (S-Sc-S junction) [52, 53] or through quantum point contacts [54, 55]. The

critical current was predicted to be quantized in units of $e\Delta/\hbar$ analogously to the quantization of the normal state conductance in ordinary quantum point contacts. Another example is the excess low-voltage conductance due to Andreev scattering in Nb-InGaAs (S-Sc) junctions [56].

Electron-electron interactions in the normal metal modify the proximity effect, both qualitatively and quantitatively [41]. If the interactions between the electrons are repulsive, the induced pair amplitude in N decays faster than in the noninteracting case. This is because interactions scatter the two electrons out of their initial, time-reversed state. If the interaction is attractive, e.g. if N becomes superconducting at a lower transition temperature, $T_{\rm cN} < T < T_{\rm cS}$, the pair amplitude decays slower because of the presence of superconducting correlations, and ξ_T diverges at $T_{\rm cN}$. A perturbative treatment of the interactions [57] shows that an additional contribution to the supercurrent arises. Its sign depends on the nature of the interactions in the slab (attractive or repulsive), and its phase-dependence has period π (in contrasts to 2π in the non-interacting case). In the tunneling regime, if the dimensions of the normal metal and its electric capacitance are small, the phenomenological capacity model described in section 2 can be used. In this case the critical current of an S-N-S system depends strongly on charging effects and can be tuned by a gate voltage applied to the island [37].

In low-dimensional semiconductor nano-structures with low electron concentration the Coulomb interactions cannot be treated as a weak perturbation. Rather a non-perturbative, microscopic treatment of interactions is required. For 1D systems, e.g. in a 2DEG gated to form a quantum wire, this can be done in the framework of the Luttinger liquid (LL) model [58]. Hybrid superconductor - Luttinger liquid (S-LL) systems are interesting since they enable one to study how the Coulomb interaction influences the phase-coherent propagation of *two* electrons through a 1D normal region. The Josephson current through a S-LL-S device has been evaluated in Refs. [59, 60]. Due to the interactions the Andreev current in a junction between a superconductor and a chiral Luttinger liquid depends in a nonlinear way of the voltage [61]. Recently also the single particle properties (DOS) of a LL connected to a superconductor have been studied, where the combined effect of interaction and Andreev tunneling leads to a behavior compared which differs qualitatively from that of an isolated LL [62].

Various theoretical approaches have been employed to study SN heterostructures. One school generalizes the scattering approaches of Landauer to include Andreev tunneling. In this case the Bogoliubov-de Gennes equations are used to construct the scattering matrix (the interested reader is invited to read the reviews on the topic [39, 40]). Another school uses quasiclassical methods starting from the Eilenberger equations (or the Usadel equations for dirty metals) with the inclusion of the appropriate boundary

conditions for the Green's functions at the interface. The two complementary methods provide a framework to tackle various problems involving hybrid structures. The quasiclassical methods have been useful to extract analytic results in the diffusive limits. On the other hand the scattering approach is more appropriate in multi-terminal geometries or in the regimes where neither the ballistic nor the diffusive limit are appropriate. In this case numerical solutions have been worked out. The next sections are devoted to a summary of the two approaches. In the final part of this chapter we discuss the influence of interactions on the proximity effect in superconductor - Luttinger liquid systems.

3.2. SCATTERING THEORY

Transport properties of mesoscopic systems have been described successfully within the scattering (Landauer) formalism [63]. The conductance is related to the transmission, and the transport theory is reduced to an analysis of the properties of the scattering matrix. This approach has been generalized to systems containing SN interfaces by Lambert [64] and Beenakker [65].

We consider an n-terminal geometry where the n-th reservoir is superconducting (the case of two or more superconducting reservoirs can be described in the same fashion). Each lead contains N incoming and outgoing modes (for simplicity we assume here that N is the same for each reservoir). In the scattering approach, one needs to evaluate the S-matrix, defined as

$$\underline{O}_\alpha = \hat{S}_{\alpha\beta}\underline{I}_\beta \ . \tag{51}$$

Here $\alpha \equiv (a,p)$ and $\beta \equiv (b,q)$, $a,b = 1,...n$ refer to the reservoirs while $q,p = 1,...N$ refer to the channel indices. The superconducting reservoir is characterized by the pair $(n, l = 1,...N)$ and it will be denoted by the index s. In Eq. (51) $\underline{O}$ and $\underline{I}$ are the amplitudes of outgoing and incoming channels, respectively. The underline denotes the two components in particle - hole space (in the absence of the superconductor the S-matrix is block-diagonal in this space).

The aim of this section is to express the scattering matrix $\hat{S}_{\alpha\beta}$ as a function of the scattering in the mesoscopic region and the scattering which takes place at the SN-interface. In order to pursue this scheme, it is conceptually simpler to separate the scattering in the normal region, which is determined by the geometry and disorder in the the mesoscopic conductor, from the scattering at the SN interface, where the Andreev processes occur. For this purpose it is assumed that a normal region, free of disorder, lies between the scattering region and the SN boundary, as illustrated in

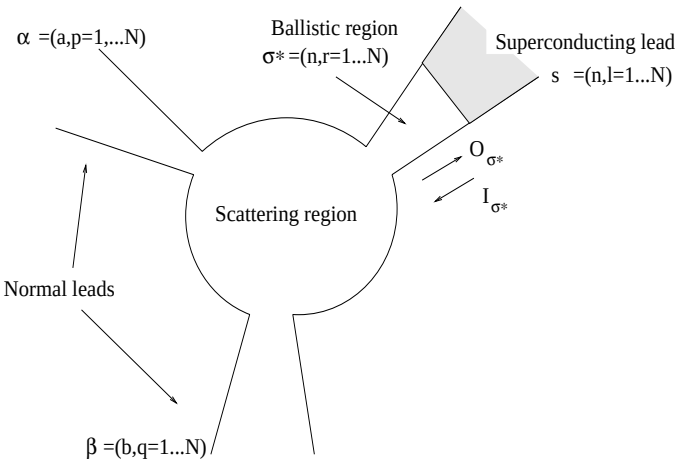

Figure 8. Sketch of the scattering region including the small ballistic region in contact with the superconducting reservoir.

Fig. 8. This ballistic region can be thought of as arbitrarily small, and its properties do not appear in the physical results.

If the superconductor were not present the scattering matrix is determined exclusively by the geometry of the mesoscopic region

$$\underline{O}_\alpha = \hat{S}^{(0)}_{\alpha\beta}\underline{I}_\beta \ . \tag{52}$$

On the other hand, the scattering at the SN interface is described by the 2×2 matrix

$$\begin{pmatrix} \underline{I}_{\sigma^\star} \\ \underline{O}_s \end{pmatrix} = \begin{pmatrix} \hat{S}^{(A)}_{\sigma^\star\sigma^\star} & \hat{S}^{(A)}_{\sigma^\star s} \\ \hat{S}^{(A)}_{s\sigma^\star} & \hat{S}^{(A)}_{ss} \end{pmatrix} \begin{pmatrix} \underline{O}_{\sigma^\star} \\ \underline{I}_s \end{pmatrix} \ , \tag{53}$$

where the index $\sigma^\star \equiv (n, r = 1, ..N)$ refers to the intermediate ballistic region, separating the scattering region from the superconducting reservoir (see Fig.8). The components of the Andreev scattering matrix are constructed by solving the Bogoliubov - de Gennes equations [66, 67]. Note also that the outgoing states in the previous equation are $\underline{I}_{\sigma^\star}$ and $\underline{O}_S$, since the incoming wave in the reservoir n (as defined in Eq. (51)) is outgoing with respect to the SN interface.

Using Eq. (52) and Eq. (53) it is possible is to eliminate $\underline{I}_{\sigma^\star}$ and $\underline{O}_{\sigma^\star}$,

which allows us to express $\hat{S}_{\alpha\beta}$ in terms of $\hat{S}^{(0)}_{\alpha\beta}$ and $\hat{S}^{(A)}_{\alpha\beta}$

$$\begin{aligned}
\hat{S}_{\alpha\beta} &= \hat{S}^{(0)}_{\alpha\beta} + \hat{S}^{(0)}_{\alpha\sigma\star}\left[\mathbf{1} - \hat{S}^{(A)}_{\sigma\star\sigma\star}\hat{S}^{(0)}_{\sigma\star\sigma\star}\right]^{-1}\hat{S}^{(A)}_{\sigma\star\sigma\star}\hat{S}^{(0)}_{\sigma\star\beta} \qquad (a,b\neq n)\\
\hat{S}_{\alpha s} &= \hat{S}^{(0)}_{\alpha\sigma\star}\left[\mathbf{1} - \hat{S}^{(A)}_{\sigma\star\sigma\star}\hat{S}^{(0)}_{\sigma\star\sigma\star}\right]^{-1}\hat{S}^{(A)}_{\sigma\star s} \qquad (a\neq n)\\
\hat{S}_{s\beta} &= \hat{S}^{(A)}_{s\sigma\star}\hat{S}^{(0)}_{\sigma\star\beta} + \hat{S}^{(A)}_{s\sigma\star}\hat{S}^{(0)}_{\sigma\star\sigma\star}\left[\mathbf{1} - \hat{S}^{(A)}_{\sigma\star\sigma\star}\hat{S}^{(0)}_{\sigma\star\sigma\star}\right]^{-1}\hat{S}^{(A)}_{\sigma\star\sigma\star}\hat{S}^{(0)}_{\sigma\star\beta} \qquad (b\neq n)\\
\hat{S}_{ss} &= \hat{S}^{(0)}_{ss} + \hat{S}^{(A)}_{s\sigma\star}\hat{S}^{0}_{\sigma\star\sigma\star}\left[\mathbf{1} - \hat{S}^{(A)}_{\sigma\star\sigma\star}\hat{S}^{(0)}_{\sigma\star\sigma\star}\right]^{-1}\hat{S}^{(A)}_{\sigma\star s}
\end{aligned} \tag{54}$$

The previous expressions for the S-matrix have a simple physical meaning: By expanding the denominators one can identify each term of the series as a sequence of scattering processes (reflections and transmissions) at the various reservoirs.

The final step is to express physical quantities in the scattering formalism. Let us first consider the current operator in the (normal) lead α

$$\hat{I}_\alpha = \frac{e}{2mi}\mathrm{Tr}\int dy_\alpha\, \underline{\Psi}_\alpha(\vec{r}_\alpha)\sigma_z\nabla\underline{\Psi}^\dagger_\alpha(\vec{r}) - \text{h.c.}\,. \tag{55}$$

Here a trace is performed in Nambu and spin space, and the matrix σ_z accounts for the different signs of the current in the electron and hole channels. The integration is over the transverse coordinate y_α in lead α. Using scattering states [68, 69] as a (more convenient) basis, with destruction and creation operators a and $a^\dagger$ of incoming scattering states, the current can be expressed as

$$\hat{I}_\alpha(t) = e\sum_{\beta\gamma}\int dE dE'\, \underline{a}^\dagger_\beta(E)\hat{\sigma}_z\left[\delta_{\alpha\beta}\delta_{\alpha\gamma} - \hat{S}^\dagger_{\alpha\beta}\hat{S}_{\alpha\gamma}\right]\underline{a}_\gamma(E')e^{-i(E-E')t}. \tag{56}$$

Since the reservoirs are in thermal equilibrium, the occupation probabilities of the scattering states are given by Fermi distributions. Combining Eq. (56) with the expressions Eq. (54) one arrives at the desired result for the transport properties in terms of the geometric properties of the scattering region and the Andreev scattering at the boundary with the superconducting lead.

In a two terminal geometry, where $\alpha \equiv (1, q = 1...N)$ is the index for the normal contact and $s \equiv (2, p = 1...N)$ for the superconductor, the average current is

$$I_{\mathrm{NS}} = 2\pi e\int dE\,[f(E) - f(E+eV)]\left\{1 - |S^{(\mathrm{ee})}_{\alpha\alpha}|^2 + |S^{(\mathrm{he})}_{\alpha\alpha}|^2\right\}\,. \tag{57}$$

A trace over the channels is implied. The current depends on the reflection coefficients. Note that the normal reflection (ee) and Andreev reflection

(he) enter with opposite sign. If there is no potential barrier at the NS interface, at energies below the gap there is no normal reflection but only Andreev reflection. The linear conductance in this regime has been obtained by Beenakker [65]

$$G_{\rm NS} = \frac{4e^2}{h} \sum_{q=1,N} \frac{T_q^2}{(2-T_q)^2} \ . \tag{58}$$

This result is the multi-terminal generalization of the formula obtained by Blonder, Tinkham and Klapwijk [66] and by Shelankov [67]. The amplitudes T_q are the eigenvalues of the geometrical transmission matrix $(S_{12}^{(0)})$, i.e. the same coefficients which enter in the multichannel Landauer formula $G = (2e^2/h) \sum_q T_q$, and the index q runs over the transverse channels in the normal lead. Various applications of the previous expression and extensions can be found in Ref. [39]. The general formula for the current beyond the Andreev approximation and at finite voltage has been discussed in Refs. [70, 71], extensions to d-wave superconductors have been considered in Ref. [72]. The use of the scattering approach is not limited to the study of the average current. Eq. (56) also allows the evaluation of the current noise (see the chapter by de Jong and Beenakker in this volume).

3.3. QUASICLASSICAL APPROACH

3.3.1. *Equilibrium Theory*

A complementary approach, developed to study hybrid structures, employs Green's functions

$$\mathcal{G}(\vec{r},\vec{r'},t) = -{\rm i}\langle T\psi(\vec{r},t)\psi^\dagger(\vec{r'},0)\rangle, \quad \mathcal{F}(\vec{r},\vec{r'},t) = -{\rm i}\langle T\psi(\vec{r},t)\psi(\vec{r'},0)\rangle \ . \tag{59}$$

Despite their apparent simplicity, the Gor'kov equations governing the dynamics of $\mathcal{G}$ and $\mathcal{F}$ are almost impossible to handle in inhomogeneous situations. On the other hand, the information contained in these equations is redundant, since usually only properties close to the Fermi energy are interesting. It is possible in these cases to reduce the Gor'kov equations to transport-like equations which are much easier to study. These are the Eilenberger [73] and Usadel [74] equations for clean and dirty systems, respectively.

The main steps are as follows. It is convenient to introduce the center of mass $\vec{R} = (\vec{r}+\vec{r'})/2$ and relative coordinates $\vec{\rho} = \vec{r}-\vec{r'}$ and to consider the Fourier transform of the Green's functions with respect to the latter (since we are dealing with time-independent situations we use the energy representation). The Green's function show strong oscillations as a function of the relative coordinate on the scale of the Fermi wavelength $\lambda_{\rm F}$. If one is interested only in variations on scales much larger than $\lambda_{\rm F}$ it is sufficient to

consider the quasiclassical Green's functions obtained by integrating $\mathcal{G}, \mathcal{F}$ over $\xi_p = p^2/2m - \mu$,

$$\left\{ \begin{array}{c} g \\ f \end{array} \right\} (E, \vec{R}, \vec{v}_{\rm F}) = \frac{\rm i}{\pi} \int d\xi_p \int d^3\rho \left\{ \begin{array}{c} \mathcal{G} \\ \mathcal{F} \end{array} \right\} (E, \vec{R}, \vec{\rho}) {\rm e}^{-{\rm i}\vec{p}\cdot\vec{\rho}} \ . \qquad (60)$$

Further simplifications are possible if the system is dirty and the dependence on the direction of $\vec{v}_{\rm F}$ is weak (the system is nearly isotropic). In this case g and f can be expanded in spherical harmonics, $g(E, \vec{R}, \vec{v}_{\rm F}) = G(E, \vec{R}) + \vec{v}_{\rm F} \cdot \vec{G}(E, \vec{R})$ and $f(E, \vec{R}, \vec{v}_{\rm F}) = F(E, \vec{R}) + \vec{v}_{\rm F} \cdot \vec{F}(E, \vec{R})$. An expansion yields the Usadel equation

$$-{\rm i}EF - \Delta G = \frac{D}{2} \left[G\hat{\nabla}^2 F - F\nabla^2 G \right] \ . \qquad (61)$$

Inelastic interactions can be accounted for by the shift $-{\rm i}E \rightarrow -{\rm i}E + 1/(2\tau_{\rm in})$, by the inelastic scattering rate. Pair-breaking effects add a further term $(1/\tau_{\rm s})GF$ on the left hand side. The magnetic field is introduced through the gauge invariant derivative, $\hat{\nabla} \rightarrow \nabla - 2ie\vec{A}$, acting on F.

The diagonal and off-diagonal component satisfy a normalization condition, $G^2 + F^2 = 1$, which is automatically guaranteed if we choose a parameterization $F = \sin\theta$ and $G = \cos\theta$.

The formalism is completed by the self-consistency equation for the gap

$$\Delta(\vec{r}) \ln \frac{T}{T_c} = 2\pi T \sum_{\omega_\mu > 0} \left[F({\rm i}\omega_\mu, \vec{r}) - \frac{\Delta(\vec{r})}{\omega_\mu} \right] \ . \qquad (62)$$

We further have to specify the boundary conditions at the SN interface (which we assume to be located in the $x = 0$ plane). In the absence of an extra boundary potential these read [75]

$$\begin{aligned} F(E, 0_{\rm S}) &= F(E, 0_{\rm N}) \\ \sigma_{\rm S} \frac{\rm d}{{\rm d}x} F(E, 0_{\rm S}) &= \sigma_{\rm N} \frac{\rm d}{{\rm d}x} F(E, 0_{\rm N}) \ . \end{aligned} \qquad (63)$$

Hence, the parameter which describes the properties of the interface is the ratio of the coherence lengths over the ratio of the conductivities in the two materials , $= \sigma_{\rm N}\xi_{T{\rm S}}/\sigma_{\rm S}\xi_{T{\rm N}}$.

This semiclassical approach has recently been applied to study the local density of states (DOS) in hybrid structures [51]. Earlier theoretical treatments of this problem can be found in Refs. [76, 77]. Experimentally the DOS is studied by attaching several tunnel junctions at certain distances from the interface and measuring the I-V characteristics [50].

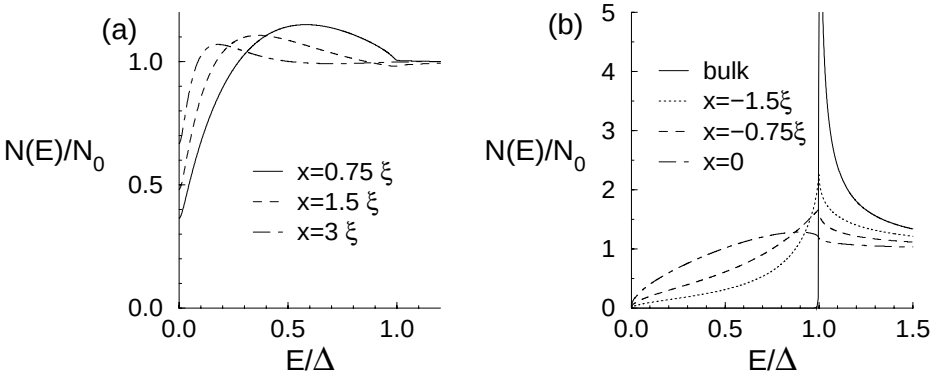

Figure 9. The density of states on the normal (a) and superconducting side (b) of a NS heterostructure at different distances from the interface. The length scale is $\xi = \sqrt{D/2\Delta}$. A nonzero pair breaking strength $1/\tau_s = 0.03\Delta$ and , $= 1$ have been assumed. From Ref. [51].

The local DOS is defined through the retarded one-electron Green's function $\mathcal{G}^{\mathrm{R}}(x,x';t) \equiv -\mathrm{i}\langle\{\psi(x,t),\psi(x',0)^\dagger\}\rangle\,\theta(t)$ as

$$N(x,E) = -\frac{1}{\pi}\,\mathrm{Im}\int_{-\infty}^{\infty} \mathrm{d}t\, e^{\mathrm{i}Et}\,\mathcal{G}^{\mathrm{R}}(x,x;t) = N(0)\,\mathrm{Re}\,G(E)\ . \qquad (64)$$

If the metal is a Fermi liquid the DOS is almost featureless $\sim N(0)$ while in the superconductor it behaves like $N(E) = N(0)E/\sqrt{E^2-\Delta^2}$. This raises the question how the DOS behaves close to an NS interface to interpolate between these two very different limits.

Due to the proximity effect, the DOS indeed acquires nontrivial structure. Results are shown in Fig. 9 (a) for the normal side of the interface. It shows a subgap structure (a bump) and a depression close to the Fermi energy. These features tend to disappear when one moves away from the interface. In the absence of pair breaking the DOS vanishes at the Fermi level. On the superconducting side the singularity at Δ is suppressed and a finite DOS appears also at low energies, as shown in Fig. 9 (b).

If the dimensions of the normal metal are finite (a slab of thickness L), a true gap E_{g} appears in the DOS of the normal metal. This mini-gap scales with the length and is related to the Thouless energy D/L^2. A fit to the numerical results is

$$E_{\mathrm{g}} \sim (\xi + L)^{-2}\ ,$$

where $\xi = \sqrt{D/2\Delta}$, implying that the effective diffusion length is $\sim \xi + L$.

3.3.2. *Nonequilibrium Situations*

To describe systems with a finite applied voltage, the formalism of nonequilibrium superconductivity [78, 79, 80] should be used. It is based on the real-time Keldysh technique [80, 81], which involves matrix Green's functions

$$\check{G} = \begin{pmatrix} \hat{G}^{\mathrm{R}} & \hat{G}^{\mathrm{K}} \\ 0 & \hat{G}^{\mathrm{A}} \end{pmatrix} \tag{65}$$

having retarded, advanced and Keldysh (R,A,K) components. Each of these are 2×2 matrices in Nambu space typical for superconductivity

$$\hat{G} = \begin{pmatrix} G & F \\ F^{\dagger} & -G \end{pmatrix}, \tag{66}$$

whose entries are quasiclassical Green's functions, which in the dirty limit satisfy the Usadel equation (61). The boundary conditions for Keldysh Green's functions at NS-interfaces have been derived by Zaitsev [82]. Applications to diffusive NS heterostructures have been discussed by Volkov *et al.* [83].

As an example, and application of the Keldysh technique, we consider the transport through a diffusive wire of length L connected to a normal and a superconducting reservoir via metallic contacts. One of the striking effects in the transport of this system is the *non-monotonic* temperature dependence when the temperature is of the order of the Thouless energy $E_L = D/L^2$. The resistance of this system initially decreases when the temperature is lowered but approaches again the normal state resistance at $T = 0$. This effect was analyzed theoretically in Refs. [49, 84, 85] and experimentally in Ref. [43].

The differential conductance, normalized to its value if the superconductor was not present, can be expressed as

$$G_{\mathrm{N}} = \frac{1}{2T} \int_0^{\infty} \mathrm{d}E \frac{D(E)}{\cosh^2(E/2T)} \tag{67}$$

where $D(E)$ is the effective energy-dependent transparency to be determined microscopically from the quasiclassical equations. It is the presence of the electric field combined with the proximity effect which renders this situation a nonequilibrium one.

At temperatures much lower than the Thouless energy E_L the conductance increases quadratically with temperature

$$G_N = 1 + A \left(\frac{T}{E_L} \right)^2 , \tag{68}$$

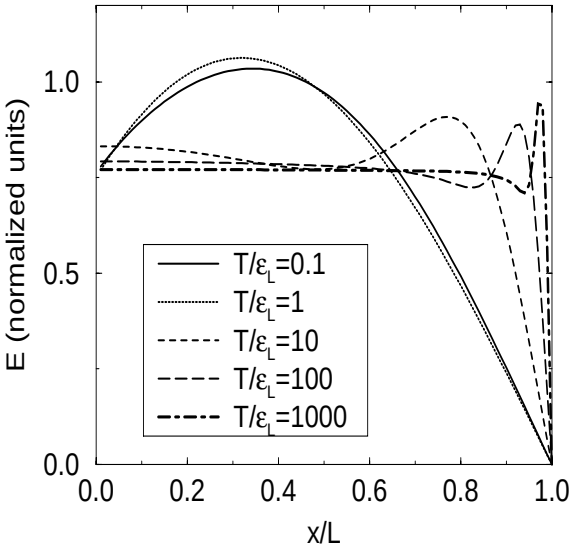

Figure 10. Electric field in the normal bridge between a bulk superconductor ($x \geq L$) and a bulk normal metal ($x \leq 0$). From Ref. [85].

where A is a constant. Although the low-temperature conductance coincides with the normal state value, the wire is influenced by the superconductor, as can be seen in the local density of states [85]. At higher temperatures $T > E_L$ the conductance decreases with rising temperature

$$G_N = 1 + B\sqrt{\frac{E_L}{T}}\ , \tag{69}$$

where B is a constant. In this regime the coherence length ξ_T in the normal wire is shorter than L. Hence the resistance of the structure is determined by the portion of the wire, $\sim L - \xi_T$, which is still normal [85].

In the non-equilibrium situation considered here, it is essential to analyze the penetration of the electrical field in the wire. This problem was considered in Ref. [86] for the infinite wire case and in Ref. [85] for the case where the wire is attached to two reservoirs. At high temperatures, the field is essentially constant, but at low temperatures it has a non-monotonic behavior. This in turn is responsible for the non-monotonic temperature dependence of the conductance. The electric field in the wire is plotted in Fig. 10.

In the presence of tunnel barriers with resistance larger than the Drude resistance of the wire, the electric field is confined to the barrier. In this

case the nonequilibrium effects related to the electric field in the wire, and responsible for the non-monotonic temperature dependence disappear.

Recent experiments [47, 48] have also studied more complex NS structures where supercurrents can flow between at least two superconducting reservoirs [47] or are induced by a magnetic flux through a loop within the structure [48]. In the picture of Andreev reflections, interference between quasiparticles acquiring a superconducting phase during the reflection process occurs. As the Usadel equations (61) describe the modulation of the Green's functions by possible gradients of the superconducting phase, the influence of these currents on the system conductance (67) can be easily calculated within the quasiclassical approach. These effects remain pronounced even at higher temperatures, when the coherence length ξ_{TN} is smaller than the geometrical lengths of the system. In this case one could expect that superconducting correlations are destroyed before interference occurs, hence the effect should be absent and supercurrents are exponentially small. However, low energy channels ($E \ll E_L$) can still interfere and contribute to the conductance with a relative weight of E_L/T. Their contribution remains pronounced. This is characteristic for linear response quantities, in contrast to thermodynamic ones like the supercurrent.

3.4. SUPERCONDUCTOR-LUTTINGER LIQUID SYSTEMS

As discussed already in the first part of this chapter, electron-electron interaction plays an important role in systems of reduced dimensionality. The interplay of proximity effect and charging was discussed in [36]. Another class of systems in which interaction is of fundamental important is that of quantum wires. In this case the capacitance model cannot applied any longer, instead a paradigm model for interacting one-dimensional electron systems is the Luttinger model (see the chapter by Fisher and Glazman in this volume for an introduction) In this last section we briefly review some properties of hybrid systems of superconductors and a Luttinger liquid. In 1D, interactions have drastic consequences. For instance, there are no fermionic quasiparticle excitations, and the transport properties cannot be described in terms of the conventional Fermi-liquid approach. Instead the low-energy excitations of the system are independent long-wavelength oscillations of the charge (ρ) and spin density (σ), which propagate with different velocities. For a quantum wire with an arbitrarily small barrier this leads to a complete suppression of transport at low energies [87, 88, 89].

Hybrid S-LL have been studied in the two extremes of tunneling junction and of perfectly transparent interfaces. In the first case the tunneling Hamiltonian is used [59], while in the second case a new type of bosonization developed in Ref. [60] is employed. In this section we consider only

the tunneling density of states in a LL with a highly transparent S-LL interface [62].

The Hamiltonian of a LL can be written in bosonized form as

$$\hat{H}_L = \frac{1}{2}\sum_j v_j \int dx \left[\frac{g_j}{2}(\nabla\theta_j)^2 + \frac{2}{g_j}(\nabla\phi_j)^2\right] , \tag{70}$$

where $j = \rho, \sigma$, and $v_j = (2/g_j)v_F$ are the renormalized interaction-dependent Fermi velocities for charge and spin density excitations. For repulsive, spin-independent interactions we have $g_\rho < 2$ and $g_\sigma = 2$. The Fermi field operators are decomposed in right- and left-moving Fermion operators $\psi_{+,s}$ and $\psi_{-,s}$, respectively, $\psi_s = e^{ik_F x}\psi_{+,s} + e^{-ik_F x}\psi_{-,s}$, where k_F is the Fermi wave vector. The fields $\psi_{\pm,s}$ in turn can be expressed through Boson operators

$$\psi^\dagger_{\pm,s} = \sqrt{\rho_0}e^{i\sqrt{\pi}[\mp\phi_s(x)+\theta_s(x)]}, \tag{71}$$

where $\theta_s = \frac{1}{\sqrt{2}}(\theta_\rho + s\theta_\sigma)$ and $\phi_s = \frac{1}{\sqrt{2}}(\phi_\rho + s\phi_\sigma)$. The density of electrons per spin in the LL is $\rho_0 = k_F/2\pi$. The fields θ, ϕ can be decomposed in a normal mode expansion which incorporates the boundary conditions at the S-LL interfaces. For a LL coupled to two superconductors at a distance L, Maslov *et al.* [60] obtained the result

$$\theta_\rho(x) = \sqrt{\frac{\pi}{2}}(J+\chi)\frac{x}{L} + i\sqrt{\frac{2}{g_\rho}}\sum_{q>0}\gamma_q \sin(qx)(\hat{b}^\dagger_{\rho,q} - \hat{b}_{\rho,q}); \tag{72}$$

$$\theta_\sigma(x) = \frac{1}{\sqrt{\pi}}\theta^{(0)}_\sigma + \sqrt{\frac{2}{g_\sigma}}\sum_{q>0}\gamma_q \cos(qx)(\hat{b}^\dagger_{\sigma,q} + \hat{b}_{\sigma,q}); \tag{73}$$

$$\phi_\sigma(x) = \sqrt{\frac{\pi}{2}}M\frac{x}{L} + i\sqrt{\frac{g_\sigma}{2}}\sum_{q>0}\gamma_q \sin(qx)(\hat{b}^\dagger_{\sigma,q} - \hat{b}_{\sigma,q}); \tag{74}$$

$$\phi_\rho(x) = \frac{1}{\sqrt{\pi}}\phi^{(0)}_\rho + \sqrt{\frac{g_\rho}{2}}\sum_{q>0}\gamma_q \cos(qx)(\hat{b}^\dagger_{\rho,q} + \hat{b}_{\rho,q}) \ . \tag{75}$$

Here, $\hat{b}^{(\dagger)}_{j,q}$ are Bose operators and $\gamma_q = \exp\{-q\alpha/2\pi\}/\sqrt{qL}$ where α is a short range cut-off. The expansion (72) – (75) is valid at energies smaller than the superconducting gap Δ. The phase difference between the two superconductors is χ; J and M describe topological excitations satisfying the constraint $J+M =$ odd. Finally, $\theta^{(0)}_\sigma$ and $\phi^{(0)}_\rho$ are canonically conjugate to M, J. The local density of states (per spin) of the LL measured at a distance x from the superconducting contact is related to the retarded one-electron Green's function of the LL by Eq. (64).

As an example we discuss the space and frequency dependent DOS of a LL contacted at $x = 0$ with a superconductor. This corresponds to the limit

$L \to \infty$ in the mode expansion given by Eqs. (72) – (75). In this case only the non-zero modes ($q > 0$) contribute to the local DOS. The correlation function $\langle \psi_s^\dagger(x,t)\psi_s(x,0)\rangle$ can be evaluated using the boson representation Eq. (71), with the result

$$\langle \psi_s^\dagger(x,0)\psi_s(x,t)\rangle = 2\rho_0 \prod_{j=\rho,\sigma} \left(\frac{\alpha^2+(2x)^2}{\alpha^2}\right)^{\gamma_j} \left(\frac{\alpha^2}{(\alpha - iv_j t)^2}\right)^{\eta_j} \times \left[\frac{\alpha^2}{(\alpha - i(2x+v_j t))(\alpha + i(2x - v_j t))}\right]^{\gamma_j} , \quad (76)$$

at distance x from the LL-S interface. Here $\gamma_j = (g_j/16 - 1/(4g_j))$ and $\eta_j = (g_j/16 + 1/(4g_j))$. At small energies $\omega \ll \Delta$, the DOS behaves as

$$N_{S-LL}(\omega) \sim \omega^{g_\rho/4 - 1/2}. \quad (77)$$

The exponent of the DOS is negative ($g_\rho < 2$), which implies a *strong enhancement* at low energies whereas in the absence of the superconductor the DOS of the LL *vanishes* at the Fermi energy

$$N(\omega) \sim \omega^{(g_\rho + 4/g_\rho - 4)/8} . \quad (78)$$

Thus the presence of the superconductor changes the properties of the Luttinger liquid in a qualitative way. Although we consider a clean S-LL interface, backscattering is induced by the superconducting gap, which reflects low-energy electrons either directly or via (multiple) Andreev processes. The enhanced DOS as a function of frequency, Eq. (77), is schematically drawn in Fig. 11; for comparison we also show the vanishing DOS in absence of the superconductor, Eq. (78).

On the other hand, at low energies ω the enhancement of the DOS persists over large distances $x(\omega) \sim v_\rho/\omega$ from the interface. On the other hand, the induced pair amplitude in the LL, which is characteristic of the presence of the superconductor, decays as a power [60] of the distance x. This profound difference in the space dependence demonstrates that the DOS provides different information compared to the proximity effect. The reason why the DOS does not approach the well-known behavior of an Luttinger liquid far from the superconducting contact is in part related to the fact that we are considering a clean wire. In this case the states in the LL are extended and the DOS enhancement does not depend on x.

Acknowledgments

We would like to thank our colleagues with whom we had been working on the problems reviewed in this article, W. Belzig, C. Bruder, G. Falci, F. W. J. Hekking, A. Odintsov, J. Siewert, L.L. Sohn, F. K. Wilhelm, and

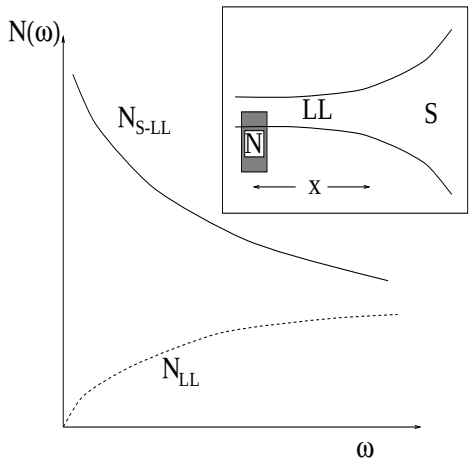

Figure 11. Schematic dependence of the DOS on frequency for a pure LL (dashed line) and for a LL connected to S (solid line). Inset: Luttinger liquid, connected adiabatically to a superconductor. The shaded area indicates a tunnel junction with a normal metal used to measure the DOS in the LL at a distance x from the interface. From Ref.[62]

A. D. Zaikin. The work has been supported by the 'Sonderforschungsbereich' 195 of the 'Deutsche Forschungsgemeinschaft'. Also the support by the A.v.Humboldt award of the Academy of Finland (G.S.) is gratefully acknowledged.

References

1. D. V. Averin and K. K. Likharev, in *Mesoscopic Phenomena in Solids*, B. L. Altshuler, P. A. Lee and R. A. Webb, eds., p. 173 (Elsevier, Amsterdam, 1991).
2. *Single Charge Tunneling*, NATO ASI Series, Vol. B 294, eds. H. Grabert and M. H. Devoret, (New York, Plenum Press 1992).
3. M. Tinkham, *Introduction to Superconductivity*, 2nd Edition, McGraw Hill (1996).
4. *Mesoscopic Superconductivity*, Proceedings of the NATO ARW, F. W. J. Hekking, G. Schön, and D. V. Averin, eds., Physica B **203** (1994).
5. C. Bruder, in *Superconductivity Review* **1**, 261 (1996).
6. G. Schön, in *Quantum Transport and Dissipation*, VCH Publishers, Chapter 4, to be published.
7. F. W. J. Hekking, L. I. Glazman, K. A. Matveev, and R. I. Shekhter, Phys. Rev. Lett. **70**, 4138 (1993).
8. F. Guinea and G. Schön, Physica B **152**, 165 (1988).
9. F. W. J. Hekking and Yu. V. Nazarov, Phys. Rev. Lett. **71**, 1625 (1993); Phys. Rev. B **49**, 6847 (1994).
10. W. Tichy, *Diplomthesis, University Karlsruhe* (1996).
11. D. V. Averin and Yu. V. Nazarov, Phys. Rev. Lett. **69**, 1993 (1992).
12. P. Lafarge, P. Joyez, D. Esteve, C. Urbina, and M. H. Devoret, Phys. Rev. Lett. **70**, 994 (1993).
13. M. T. Tuominen, J. M. Hergenrother, T. S. Tighe, and M. Tinkham, Phys. Rev. Lett. **69**, 1997 (1992); Phys. Rev. B **47**, 11599 (1993).
14. T. M. Eiles, J. M. Martinis, and M. H. Devoret, Phys. Rev. Lett. **70**, 1862 (1993).

15. J. M. Hergenrother, M. T. Tuominen, and M. Tinkham, Phys. Rev. Lett. **72**, 1742 (1994); J. M. Hergenrother et al., page 327 in Ref. 4.
16. G. Schön and A. D. Zaikin, Europhys. Lett. **26**, 695 (1994).
17. G. Schön, J. Siewert, and A. D. Zaikin, p. 340 in Ref. [4], and in *Quantum Dynamics of Submicron Structures*, NATO ASI Series B **291**, eds. H. Cerdeira, B. Kramer, and G. Schön, p. 489 (1995).
18. A. O. Caldeira and A. J. Leggett, Ann. Phys. (NY) **149**, 374 (1983).
19. U. Weiss, *Quantum Dissipative Systems*, Series in Modern Condensed Matter Physics, Vol. 2 (World Scientific, 1993).
20. U. Eckern, G. Schön, and V. Ambegaokar, Phys. Rev. B **30**, 6419 (1984).
21. G. Schön and A. D. Zaikin, Phys. Rep. **198**, 237 (1990).
22. F. W. J. Hekking, L. I. Glazman, and G. Schön, Phys. Rev. B **51**, 15312 (1995).
23. T.A. Fulton, P.L. Gammel, D.J. Bishop, L.N. Dunkleberger, and G.J. Dolan, Phys. Rev. Lett. **63**, 1307 (1989).
24. A. Maassen v.d. Brink, G. Schön, and L. J. Geerligs, Phys. Rev. Lett. **67**, 3030 (1991); A. Maassen v.d. Brink et al., Z. Phys. B **85**, 459 (1991).
25. D. B. Haviland, Y. Harada, P. Delsing, C. D. Chen, and T. Claeson, Phys. Rev. Lett. **73**, 1541 (1994).
26. J. Siewert and G. Schön, Phys. Rev. B **54**, 7421 (1996).
27. K.A. Matveev, M. Gisselfält, L. I. Glazman, M. Jonson, and R. I. Shekter, Phys. Rev. Lett. **70**, 2940 (1993); K. A. Matveev, L. I. Glazman, and R. I. Shekter, Mod. Phys. Lett. B **8**, 15 (1994).
28. P. Joyez, Ph.D. Thesis, Université Paris 6 (1995)
29. M. H. Devoret, private communication.
30. H. Schoeller and G. Schön, Phys. Rev. B **50**, 18436 (1994).
31. J. König, H. Schoeller, G. Schön, Europhys. Letters **31**, 31 (1995); J. König et al. in *Quantum Dynamics of Submicron Structures*, NATO ASI Series B **291**, eds. H. Cerdeira, B. Kramer, and G. Schön, p. 221 (1995).
32. L. I. Glazman and K. A. Matveev, Sov. Phys. JETP. **71**, 1031 (1990); K. A. Matveev, Sov. Phys. JETP **72**, 892 (1991).
33. S. V. Panyukov and A. D. Zaikin, Phys. Rev. Lett. **67**, 3168 (1991); D. S. Golubev and A. D. Zaikin, Phys. Rev. B **50**, 8736 (1994).
34. G. Falci, G. Schön, and G. T. Zimanyi, Phys. Rev. Lett. **74**, 3257 (1995); and p. 409 in [4].
35. H. Grabert, Phys. Rev. B **50**, 17364 (1994); X. Wang and H. Grabert, Phys. Rev. B **53**, 12621 (1996).
36. C. Bruder, R. Fazio, and G. Schön, Phys. Rev. B **50**, 12766 (1994); and p. 240 in [4].
37. R. Bauernschmitt, J. Siewert, A. A. Odintsov, and Yu. V. Nazarov, Phys. Rev. B **49**, 4076 (1994).
38. L. G. Aslamazov, A. I. Larkin, and Yu. N. Ovchinnikov, Zh. Eksp.Teor. Fiz. **55**, 323 (1968) [Sov. Phys. JETP **28**, 171 (1969)].
39. C.W.J. Beenakker in *Mesoscopic Quantum Physics*, edited by E. Akkermans, G. Montambaux, and J.-L Pichard (North Holland, Amsterdam) 1995.
40. C.J. Lambert and R. Raimondi, J. Phys. Cond. Matt. (to be published).
41. G. Deutscher and P. G. de Gennes, in *Superconductivity*, edited by R. D. Parks (Marcel Dekker, New York, 1965), Vol.II, p. 1005.
42. A. F. Andreev, Zh. Eksp. Teor. Fiz. **46**, 1823 (1964) [Sov. Phys. JETP **19**, 1228 (1964)].
43. P. Charlat, H. Courtois, Ph. Gandit, D. Mailly, A.F. Volkov, and B. Pannetier, Phys. Rev. Lett., to be published.
44. I.O. Kulik, Zh. Eksp. Teor. Fiz. **57**, 1745 (1969) [Sov. Phys. JETP **30**, 944 (1970)].
45. H. Pothier, S. Guéron, D. Esteve, and M. H. Devoret, in Ref[4]; Phys. Rev. Lett. **73**, 2488 (1994).
46. H. Nakano and H. Takayanagi, Sol. St. Comm. **80**, 997 (1991).

47. V.T. Petrashov, V.N. Antonov, and M. Persson, Physica Scripta **42**, 136 (1992); V.T. Petrashov, V.N. Antonov, P. Delsing, and, T. Claeson, Phys. Rev. Lett. **70**, 347 (1993); Phys. Rev. Lett. **74**, 5268 (1995).
48. H. Courtois, Ph. Gandit, D. Mailly, and B. Pannetier, Phys. Rev. Lett. **76**, 130 (1996).
49. Yu. V. Nazarov and T. H. Stoof, Phys. Rev. Lett. **76**, 823 (1996); Phys. Rev. B **53**, 14496 (1996).
50. S. Guéron, H. Pothier, N. O. Birge, D. Esteve, and M. Devoret, Phys. Rev. Lett. **77**, 3025 (1996) .
51. W. Belzig, C. Bruder, and G. Schön, Phys. Rev. B **54**, 9443 (1996).
52. J. Nitta, T. Azaki, H. Takayanagi, and K. Arai, Phys. Rev. B **46**, 14286 (1992).
53. A. Dimoulas, J. P. Heida, B. J. van Wees, T. M. Klapwijk, W. v.d. Graaf, and G. Borghs, Phys. Rev. Lett. **74**, 602 (1995).
54. C. W. J. Beenakker and H. van Houten, Phys. Rev. Lett. **66**, 3056 (1991).
55. A. Furusaki, H. Takayanagi, and M. Tsukada, Phys. Rev. Lett. **67**, 132 (1991).
56. A. Kastalsky, A. W. Kleinsasser, L. H. Greene, R. Bhat, F. P. Milliken, and J. P. Harbison, Phys. Rev. Lett. **67**, 3026 (1991).
57. B. L. Altshuler, D. E. Khmelnitskii, and B. Z. Spivak, Solid State Comm. **48**, 841 (1983).
58. J. Voit, Rep. Prog. Phys. **58**, 977 (1995).
59. R. Fazio, F.W.J. Hekking,, and A.A. Odintsov, Phys. Rev. Lett. **74**, 1843 (1995).
60. D.L. Maslov, M. Stone, P.M. Goldbart, and D. Loss, Phys. Rev. B **53**, 1548 (1996).
61. M.P.A. Fisher, Phys. Rev. B **49**, 14550 (1994).
62. C. Winkelholz, R. Fazio, F.W.J. Hekking, and G. Schön, Phys. Rev. Lett. **77**, 3200 (1996).
63. see e.g. the textbook by S. Datta, *Mesoscopic Electron Transport*, Cambridge University Press (1995).
64. C.J. Lambert, J. Phys. C **3**, 6579 (1991).
65. C.W.J. Beenakker, Phys. Rev. B **46**, 12481 (1992).
66. G.E. Blonder, M. Tinkham, and T.M. Klapwijk, Phys. Rev. B **25**, 4515 (1982).
67. A.L. Shelankov Sov. Phys. Solid St. bf 26, 981 (1984).
68. M. Büttiker, Phys. Rev. B **46**, 12485 (1992).
69. M.P. Anantram and S. Datta, Phys. Rev. B **53**, 16390 (1996).
70. G.B. Lesovik, A.L. Fauchère, and G. Blatter, Phys. Rev. B **55**, 3146 (1997).
71. J. Sánchez-Canizares and F. Sols, Phys. Rev. B **55**, 531 (1997).
72. P. Cook, R. Raimondi and C.J. Lambert, Phys. Rev. B **54**, 9491 (1996).
73. G. Eilenberger, Z. Phys. **214**, 195 (1968).
74. K. Usadel, Phys. Rev. Lett. **25**, 507 (1970).
75. M.Y. Kupriyanov and V.F. Lukichev, Zh. Eksp.Teor. Fiz. **94**, 139 (1988) [Sov. Phys. JETP **67**, 1163 (1988)].
76. W.L. McMillan, Phys. Rev. **175**, 537 (1968).
77. A.A. Golubov and M.Y. Kupriyanov, J. Low. Temp. Phys. **70**, 83 (1988).
78. A.I. Larkin and Yu.N. Ovchinnikov in *Nonequilibrium Superconductivity*, eds. D.N. Langenberg and A.I. Larkin, (Elsevier, Amsterdam, 1985).
79. A. Schmid and G. Schön, J. Low. Temp. Phys. **20**, 207 (1975).
80. A. Schmid in *Nonequilibrium Superconductivity, Phonons, and Kapitza Boundaries*, NATO ASI Series B 65, ed. K.E. Gray, (Plenum, New York 1981)
81. J. Rammer and H. Smith, Rev. Mod. Phys. **58**, 323 (1986).
82. A.V. Zaitsev, Sov. Phys. JETP **59**, 1015 (1984); M.Yu. Kuprianov and V.F. Lukichev, Sov. Phys. JETP **94**, 139 (1988).
83. A.F. Volkov, A.V. Zaitsev, and T.M. Klapwijk, Physica C **59**, 21 (1993).
84. A.F. Volkov and C.J. Lambert, J. Cond. Mat., **8**, L45 (1996).
85. A.A. Golubov, F.K. Wilhelm, and A.D. Zaikin, to be published in Phys. Rev. B.
86. F. Zhou, B. Spivak, and A. Zyuzin, Phys. Rev. B 52,4467 (1995)
87. C.L. Kane and M.P.A. Fisher, Phys. Rev. Lett. **68**, 1220 (1992).

88. K.A. Matveev and L.I. Glazman, Phys. Rev. Lett. **70**, 990 (1993).
89. A. Furusaki and N. Nagaosa, Phys. Rev. B 47,4631 (1993).